REPORT DOCUMENTATION PAGE			Form Approved OMB No. 0704-0188

1. AGENCY USE ONLY *(Leave blank)*	2. REPORT DATE	3. REPORT TYPE AND DATES COVERED
	13.Aug.03	THESIS

4. TITLE AND SUBTITLE
"COMPARISONS OF SATELLIT-DERIVED CLOUD HEIGHTS WITH RADAR MEASUREMENTS OF MID-LEVEL, MIXED-PHASE CLOUDS"

5. FUNDING NUMBERS

6. AUTHOR(S)
CAPT JONES JAMES C

7. PERFORMING ORGANIZATION NAME(S) AND ADDRESS(ES)
COLORADO STATE UNIVERSITY

8. PERFORMING ORGANIZATION REPORT NUMBER
CI02-1222

9. SPONSORING/MONITORING AGENCY NAME(S) AND ADDRESS(ES)
THE DEPARTMENT OF THE AIR FORCE
AFIT/CIA, BLDG 125
2950 P STREET
WPAFB OH 45433

10. SPONSORING/MONITORING AGENCY REPORT NUMBER

11. SUPPLEMENTARY NOTES

12a. DISTRIBUTION AVAILABILITY STATEMENT
Unlimited distribution
In Accordance With AFI 35-205/AFIT Sup 1

12b. DISTRIBUTION CODE

13. ABSTRACT *(Maximum 200 words)*

14. SUBJECT TERMS	15. NUMBER OF PAGES	16. PRICE CODE
	72	

17. SECURITY CLASSIFICATION OF REPORT	18. SECURITY CLASSIFICATION OF THIS PAGE	19. SECURITY CLASSIFICATION OF ABSTRACT	20. LIMITATION OF ABSTRACT

THESIS

COMPARISONS OF SATELLITE-DERIVED CLOUD HEIGHTS WITH RADAR MEASUREMENTS OF MID-LEVEL, MIXED-PHASE CLOUDS

Submitted by

James Cooper Jones

Department of Atmospheric Science

In partial fulfillment of the requirements

For the Degree of Master of Science

Colorado State University

Fort Collins, Colorado

Spring 2003

DISCLAIMER

The views expressed in this article are those of the author and do not reflect the official policy or position of the United States Air Force, Department of Defense, or the U.S. Government.

COLORADO STATE UNIVERSITY

April 4, 2003

WE HEREBY RECOMMEND THAT THE **THESIS** PREPARED UNDER OUR SUPERVISION BY JAMES COOPER JONES, ENTITLED "COMPARISONS OF SATELLITE-DERIVED CLOUD HEIGHTS WITH RADAR MEASUREMENTS OF MID-LEVEL, MIXED-PHASE CLOUDS" BE ACCEPTED AS FULFILLING IN PART REQUIREMENTS FOR THE DEGREE OF MASTER OF SCIENCE.

Committee on Graduate Work

_____

_____

_____

_____

_____

Adviser

_____

Department Head

ABSTRACT OF **THESIS**

COMPARISONS OF SATELLITE-DERIVED CLOUD HEIGHTS WITH RADAR MEASUREMENTS OF MID-LEVEL, MIXED-PHASE CLOUDS

Radiances from the 10.7 um channel of Geostationary Operational Environmental Satellite-8 are converted to cloud top height (CTH) for comparison to 95 GHz radar measurements of mid-level, mixed-phase clouds. CTH is objectively determined by airborne cloud radar and used as 'ground truth'. Three methods of satellite-derived CTH are compared to the radar. The black body (BB) method assumes the cloud radiates as a black body, converts the radiance to brightness temperature and height via comparison to an atmospheric sounding. Errors range from +900 m to –1200 m depending on the opaqueness of the cloud. The spatial coherence (SC) method determines a single mean value of cloud top radiance for a cloud scene and converts the radiance to height in a manner similar to the BB method. Errors range from +200 m to +900 m without much dependence on opaqueness. The optimal estimation method determines CTH using BB radiances and a SC method with an 'a priori' constraint from a sounding. The solution is determined iteratively using a perturbation method. Errors range from +200 m to +700 m with only a slight dependence on the opaqueness of the cloud until the clouds become very optically thin.

James Cooper Jones
Department of Atmospheric Science
Colorado State University
Fort Collins, Colorado 80523-1371
Spring 2003

ACKNOWLEDGEMENTS

Many thanks to my advisor, Dr. Thomas Vonder Haar, and committee members, Dr. Christian Kummerow, and Dr. V. N. Bringi. Their suggestions have been extremely helpful and their time is greatly appreciated. I also want to thank all of the Vonder Haar research group for their advice and assistance. Additional thanks are in order for many of the scientists at the Cooperative Institute for Research in the Atmosphere (CIRA) for their help, especially John Davis, Adam Kanciewicz, Kelly Dean, John Forsythe, and Larry Carey. Thanks should also go to many of my fellow classmates, with whom I worked countless hours on homework and projects. I would like to thank my children, for their love and support. Finally, I would like to thank my wife, for her unfailing support not only during this work but also throughout our 17-year marriage. Without her I would never have made it through graduate school. Funding and support for this research was supplied by the United States Air Force through the Air Force Institute of Technology, Civilian Institution program.

TABLE OF CONTENTS

LIST OF FIGURES

CHAPTER 1 - INTRODUCTION

There are many uses for accurate determination of the locations of clouds in the atmosphere. Horizontal position can easily be obtained via remote sensing by geostationary satellites. However, vertical placement by similar means poses some serious challenges. Accurate determination of vertical cloud location is needed for input to computer models, especially in areas such as oceans where surface measurements are not routinely available. Chen (1998) points out inadequate vertical resolution of rawinsonde networks in the middle troposphere as a reason to use satellite-derived cloud heights and associated moisture fields as input to models. Chen goes on to describe the difficulties encountered with assimilating these fields. A better understanding of the current capabilities of remote sensing tools could help alleviate these difficulties. Nieman (1993) describes satellite-derived cloud-motion vectors and the need for better understanding of the vertical placement of these vectors, especially when the cloud motion vectors are derived from thin clouds that are semitransparent in the infrared window wavelengths. Clothiaux et al. (1999) state the horizontal distribution of clouds is best characterized by radiometry from satellites and the vertical distribution is best measured by radar and lidar. Taking advantage of the more accurate vertical positioning of clouds by radar, this work attempts to evaluate methods of cloud top determination by geostationary satellite radiometry as compared to radar. The purpose is to quantify the

errors associated with various methods of cloud top determination and identify sources of error.

Cloud top height determination by satellite radiometry is not new. Glahn (1966) describes attempts to determine cloud top height and aerial coverage using the black body method used in this work and the problems associated with it. Since then, advances in satellite instruments have increased spatial resolution, improved signal-to-noise ratios, and added multi-spectral capability (Menzel and Purdom, 1994). However, the same sets of difficulties confront us when trying to determine cloud top height.

1.1. Data Set

The data used in this study is from the Complex Layered Cloud Experiment (CLEX). The CLEX, sponsored by the DOD Center for Geosciences and Atmospheric Research (CG/AR) at the Cooperative Institute for Research in the Atmosphere (CIRA) in collaboration with Colorado State University is an ongoing field program. It seeks a better physical understanding of mixed-phase non-precipitating clouds in the middle troposphere or *"The Forgotten Clouds"* (Vonder Haar et al. 1997). In particular, the CLEX strives to document the microphysical, dynamical, and radiative properties of these clouds with the goal of improving their forecasting, modeling and remote detection. Using in-situ aircraft observations, CLEX-5 through 8 have documented the detailed microphysical and radiative structure of mid-level clouds (Fleishauer et al., 2001, Carey et al., 2001) and have addressed the question of what causes altocumulus to decay (Larson et al., 2001). These results have provided many insights toward the better forecasting of mid-level clouds. The latest, CLEX-9, occurred in Oct-Nov of 2001. An

overview of the scientific objectives of CLEX-9 can be found in Carey et al. (2001). This study will focus on two days during CLEX-9, 14 Oct and 2 Nov.

The CLEX clouds are characterized by a mixture of ice and supercooled liquid water generally located near or above the freezing level (Fleishauer, 2001). Observations have shown these clouds to be highly variable in optical thickness resulting in large variations in the accuracy of cloud top height determinations. They do not produce severe weather and are typically ignored by researchers. However, according to Warren et al. (1988), these types of clouds cover approximately 22% of Earth's surface.

The impact of these clouds has become increasingly more significant especially to Department of Defense (DoD) operations due to increased use of lightweight remotely controlled airframes that are susceptible to ice buildup on the wings. Difficulty detecting and forecasting mid-level clouds with conventional meteorological observations and models during military operations in Southwest Asia (e.g., DESERT SHIELD/STORM, 1990-1991) is detailed in Vonder Haar et al. (1997). Extensive layers of these non-precipitating, mid-level clouds frequently masked target areas, hampered the use of uninhabited aerial vehicles (UAV's) , electro-optic sensors and weapons systems. As a result, poorly forecasted and detected mid-level clouds often forced the cancellation of refueling, intelligence and strike missions. During portions of the Balkan conflicts (1997-1998), my own frustrating experience in locating suitable aircraft holding patterns for aerial refueling, reconnaissance, and surveillance aircraft to cloud-free altitudes provided motivation for a more accurate detection of cloud tops and a more thorough understanding of the problems associated with remotely sensing these clouds.

CHAPTER 2 – INSTRUMENTATION OF CLEX

2.1. Wyoming Airborne Cloud Radar

The radar used during CLEX-9 was the University of Wyoming (UW) Cloud Radar. It is a pulsed, dual-polarization radar operating at 94.92 GHz (~3mm) with a peak power of 1.6 KW. Reflectivity measurements were made at 20 KHz with 30 m range gate spacing. Sampling was limited to 150 range gates resulting in a 4.5 Km maximum range. The radar was mounted in the UW King Air and operated in the side and upward looking modes. Details of the radar and its operation can be found in Pazmany et al.(1994). The radar data were smoothed from the 20 KHz sampling rate to 1 Hz to reduce the amount of processing time in the comparisons to satellite data which is of a much more coarse resolution.

2.2. Wyoming King Air Instrumentation

Several instruments were used to collect in-situ data during CLEX-9. The instruments were mounted on the UW King Air. Figure 2.1 shows the locations of each of the sensors.

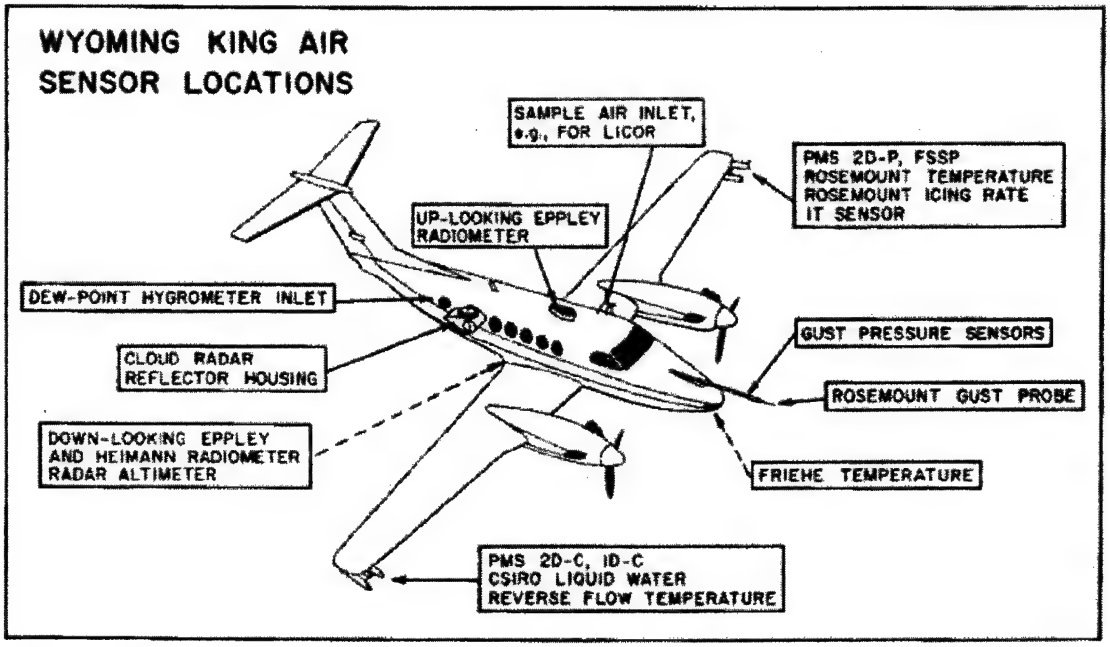

Figure 2.1. Wyoming King Air Sensor Locations

In-situ temperature measurements were taken by the Rosemount 102 and the Reverse Flow Temperature Probe. The sampling rate for both instruments was 25 Hz. The data were then smoothed to 1-second averages to match the radar data and matched in time to the radar clock. These in-situ measurements were used to verify the National Weather Service (NWS) sounding's representativeness in the cloud. When necessary the local sounding was adjusted to match the in-situ data.

Both instruments were used to verify the accuracy of the in-situ measurements. The Rosemount 102 measures the air temperature using a platinum resistance thermometer and the housing is heated to eliminate icing during flight. Because the sensing element can get wet from hydrometeors it may not give an accurate measurement in cloud or precipitation. The reverse flow temperature probe also measures air temperature using a platinum resistance thermometer, however its housing is designed so that air flows in through the back which helps keep hydrometeors from wetting the

element. Both instruments share similar characteristics of range (–50 to +50 °C) and accuracy of 0.5 °C. Measurements from both instruments were compared to ensure accuracy of in-situ temperature measurement.

Pitch and Roll were measured by the Honeywell Laserref SM Inertial Reference System (IRS). The Honeywell IRS uses ring laser gyros and accelerometers to determine aircraft position, attitude and accelerations. Output from the IRS is used to determine the pitch and roll of the aircraft and then the radar data are corrected for the geometrical errors induced by the orientation of the aircraft. The IRS has an accuracy of .05° and a resolution of .000172°.

The position and altitude of the aircraft were determined by the Trimble 2000 Differential GPS. The Trimble 2000 GPS outputs position with an accuracy of about 30 meters. All the aircraft positions used in this work (e.g. latitude, longitude, and altitude in MSL) were derived from this instrument.

Cloud microphysics measurements were made using the Rosemount 871FA Icing Detector, the Droplet Measurement Technologies Model LWC-100 Liquid Water Sensor and the Gerber PVM-100A to determine the Liquid Water Content(LWC). The Particle Measuring System(PMS) Optical Array Probe(OAP) 2-Dimentional Cloud(2D-C) was used to determine Ice Water Content (IWC). Detailed information on PMS probes can be found in NCAR's Research Aviation Facility Bulletin 24 (Baumgardner, 1989). The microphysical information was used to verify cloud tops as measured by radar. Comparisons between microphysical measurements, visual verification noted in mission logs and radar cloud tops were made to ensure the radar derived cloud top was correct.

2.3. GOES Instrumentation

GOES-8 is the Eastern operational satellite used for meteorological purposes. This study used GOES-8 to better understand the status of current capabilities in detecting and measuring cloud top heights. The sensor used was Channel 4 (10.7 um). The spectral response of the instrument is shown in Fig. 4.2.

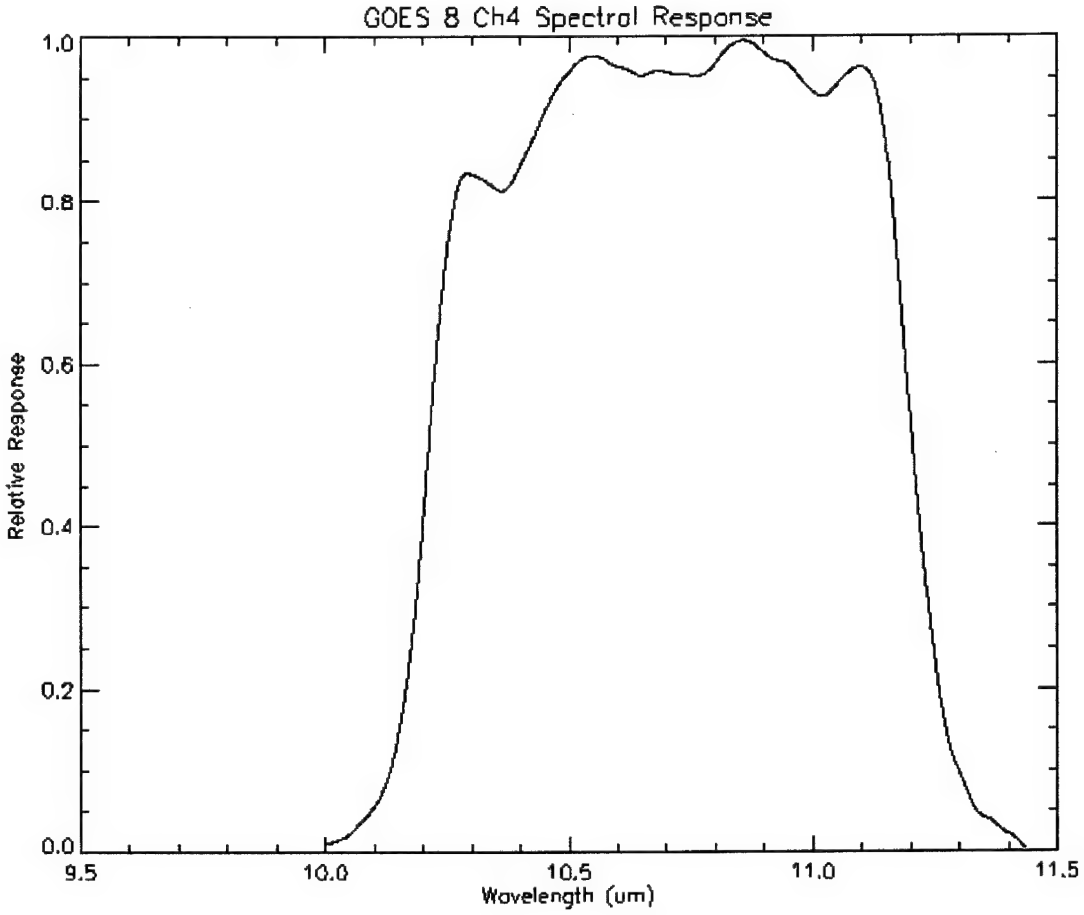

Figure 2.2. Spectral Response of GOES-8 Imager (10.7 um channel) – Data for graph courtesy of Cooperative Institute for Meteorological Satellite Studies (CIMMS)

The bandwidth ranges from 10.20 um to 11.20 um with a central wavelength of 10.7 um. The instrument has the capability to measure temperatures ranging from 4 K to 320 K with an accuracy of 1 K. For the lapse rates observed in this study (1K/100 ft), the

resulting height accuracy of cloud top is approximately +/- 100 m. The detector is made from mercury, cadmium and telluride and is arranged in a square with an instantaneous geometric field of view of 112 urad. This arrangement creates a resolution of 4 km at the suborbital point. The sensor detects radiance and in turn produces a voltage, which is digitized onboard the satellite to a 10-bit brightness count. The counts were converted to radiance and brightness temperature using GOES Variable Conversion as described by Weinreb et al.(1998). Figures 2.3 and 2.4 show the response curves for the brightness counts to radiance and temperature.

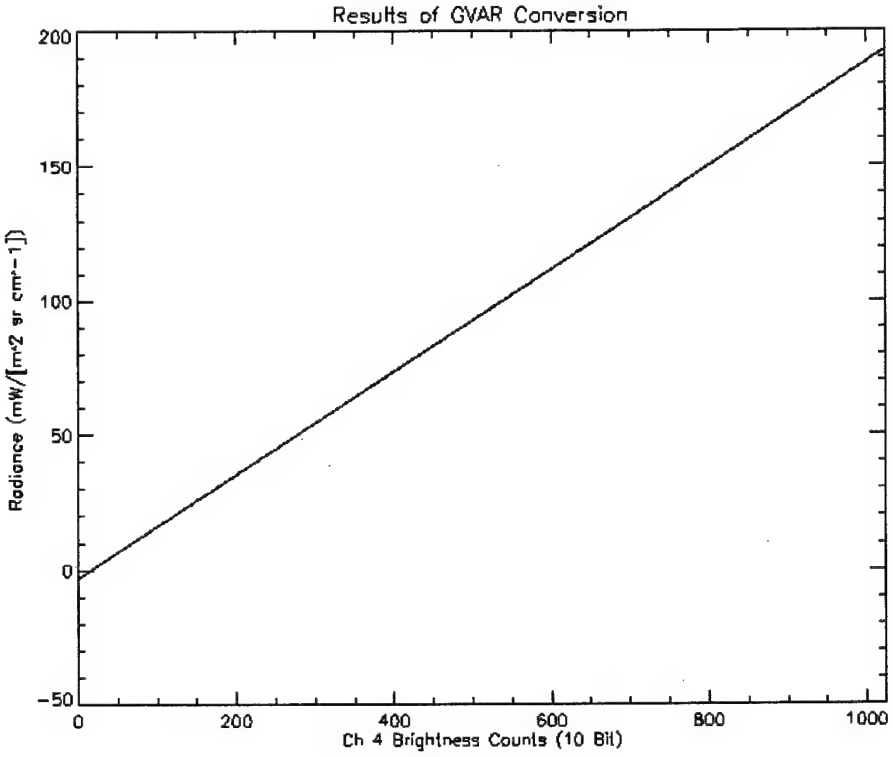

Figure 2.3. Brightness Counts to Radiance Conversion for GOES-8 10.7 um channel

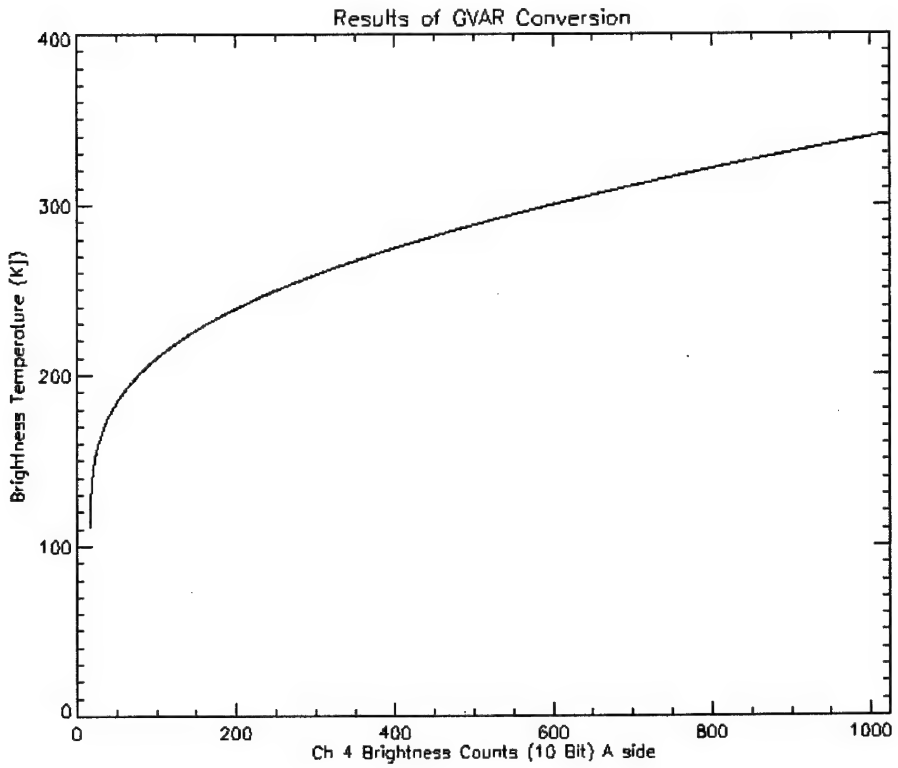

Figure 2.4. Brightness Counts to Temperature Conversion for GOES-8 10.7 um channel

CHAPTER 3 – DATA COLLECTION AND PROCESSING

3.1. Radar Reflectivity Data

Once collected, the radar data were corrected for pitch and roll and the altitude of the aircraft. Each range gate was assigned its respective distance from the aircraft and then the pitch and roll correction was applied. Since each range gate's distance from the radar is fixed, the pitch and roll of the aircraft causes an error in the actual height above sea level of the range gate. Figure 3.1 shows an example of this.

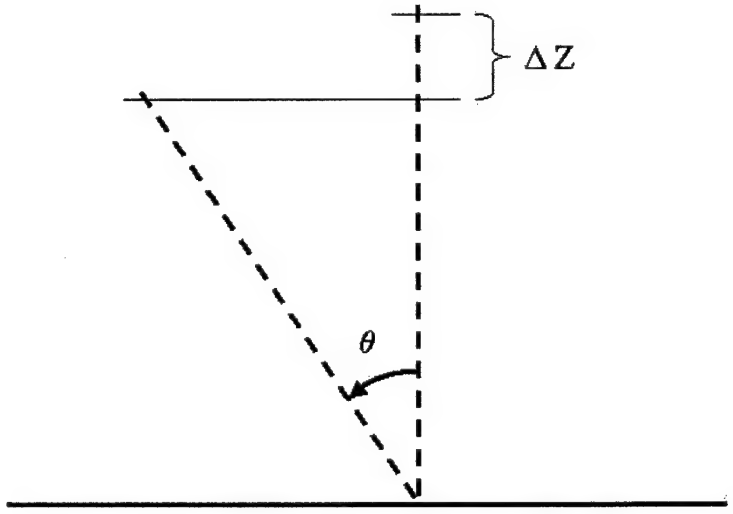

θ - Pitch or Roll Angle
ΔZ - Difference in MSL height due to pitch or roll

Figure 3.1. – Pitch or Roll Error in Range Gate Height

The correction is complicated by the fact the aircraft can pitch and roll simultaneously, but with some simple geometry one can derive the equation:

$$True\ Height = Range\ Gate\ Height * (\cos(pitch\ angle)^2 + \cos(roll\ angle)^2 - 1)^{1/2}$$

Once the true range gate heights have been established, the GPS altitude of the aircraft was added to produce an array of MSL heights for each range gate.

3.2. GOES Data

All imager data were collected as full disk images. For efficient computer processing, the coverage was reduced using the CIRA produced program SubSect. Using SubSect, the images were reduced to the CLEX-9 target region, 38.5 to 42.5 N and 104.0 to 98.0 W. This sector allowed for the monitoring of clouds in the entire CLEX-9 target region.

3.3. Alignment of Radar and Satellite Data Sets

In order to compare results of cloud top height as measured from radar and satellite, the data must be aligned spatially and temporally. This presents some difficulty to the scientist without complete control of each instrument. While GOES data was an integral part of the CLEX dataset, the satellite was not dedicated to the experiment. The GOES system runs on an automated schedule with products becoming available on a routine schedule. The satellite data are a mere 'snapshot' at a given time whereas the radar collects data in a more continuous fashion. In order to ensure cloud top comparisons are of the same cloud top, rules and limitations must be set. As a general rule, the times under consideration are when the aircraft is sampling the cloud with the radar and a definite cloud top is observed. Due to the high attenuation of 95 GHz by water particles, ideal time frames include only those where an observed cloud top occurs

within the first 50 range gates. This ensures the sensitivity of the radar is sufficient to correctly determine the cloud top. For this radar, Vali and Haimov (1998) calculated a one-way attenuation coefficient of 5.5 dB/km per g/m^3 at –10C. The liquid water contents of these clouds were approximately .5 g/m^3. Limiting the range used by the radar to detect cloud top height to 150 m results in a maximum two-way attenuation of .825 dB/km. This is more than sufficient to ensure sensitive cloud top height measurements.

Additional consideration must be made for cloud advection. To ensure the cloud doesn't modify too much from the time the satellite scans occur and the radar samples the cloud, only about 7.5 to 10 minutes of radar data are compared to the satellite data both before and after the stamped time of the image. This yields 15 to 20 minutes of radar sampling per satellite image.

To match the data sets spatially, a nearest neighbor routine is used. The latitude and longitude for each 1 second scan of radar data are obtained from the GPS. These positions are compared to the available fields of view (FOV) from the matching satellite image. A least squares differencing method is applied to locate the closest FOV to each scan of radar data.

Parallax, the error caused by an observational position that provides a line of sight other than directly overhead, is an additional consideration. Since the center point of each FOV is assigned a latitude and longitude that corresponds to a point on the earth's surface, elevated objects in the line of sight 'appear' in one FOV but actually physically reside in another. Figure 3.2 shows a graphical representation.

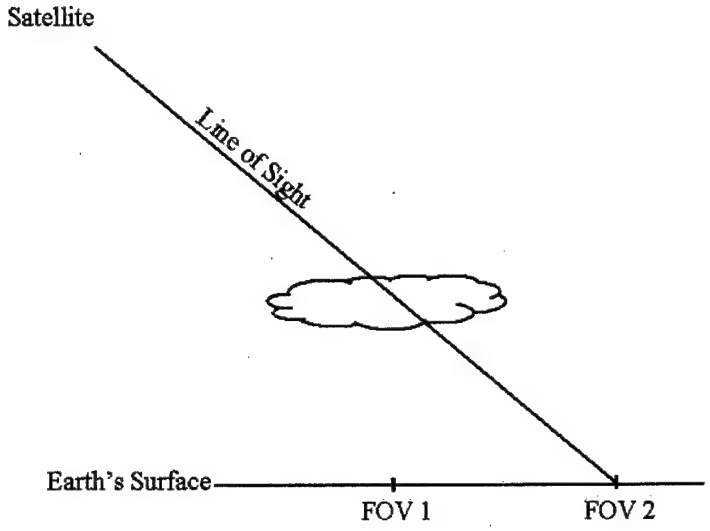

Figure 3.2. Parallax Caused by Non-Overhead Line of Sight

In this example the cloud is observed by the satellite to reside in FOV 2. However, the cloud is physically located directly over FOV 1. In this study, the majority of the observed clouds are located at approximately 3-5 Km MSL. Considering satellite zenith angles of 45 to 50 degrees over the experimental area and FOVs approximately 4 Km wide, the position of the cloud-filled FOV's could in error by a maximum of one FOV. Since the observed cloud fields predominantly displayed limited vertical variability no correction for parallax has been made in the present study.

CHAPTER 4 – CLOUD TOP HEIGHT DETERMINATION

4.1. Radar Derived Cloud Heights

Once the data sets are aligned it is possible to compare the results of various methods of determining cloud top heights. The method chosen to objectively determine the top of a cloud by radar is based on a reflectivity threshold. The threshold is determined by a histogram method and then a binary cloud mask is created. The cloud mask makes the distinction between cloud-filled and cloud-free range gates. Searching from the first range gate upward to the first cloud-free range gate yields the range gate where cloud top occurs. The height of the range gate becomes the cloud top height. The following paragraphs describe the method in more detail.

First, the radar data were sectioned into ~15 minute arrays with each element of the array representing the 1-second average of reflectivity for the range gate. Figure 4.1 shows radar reflectivity array from the 2 Nov 01 case.

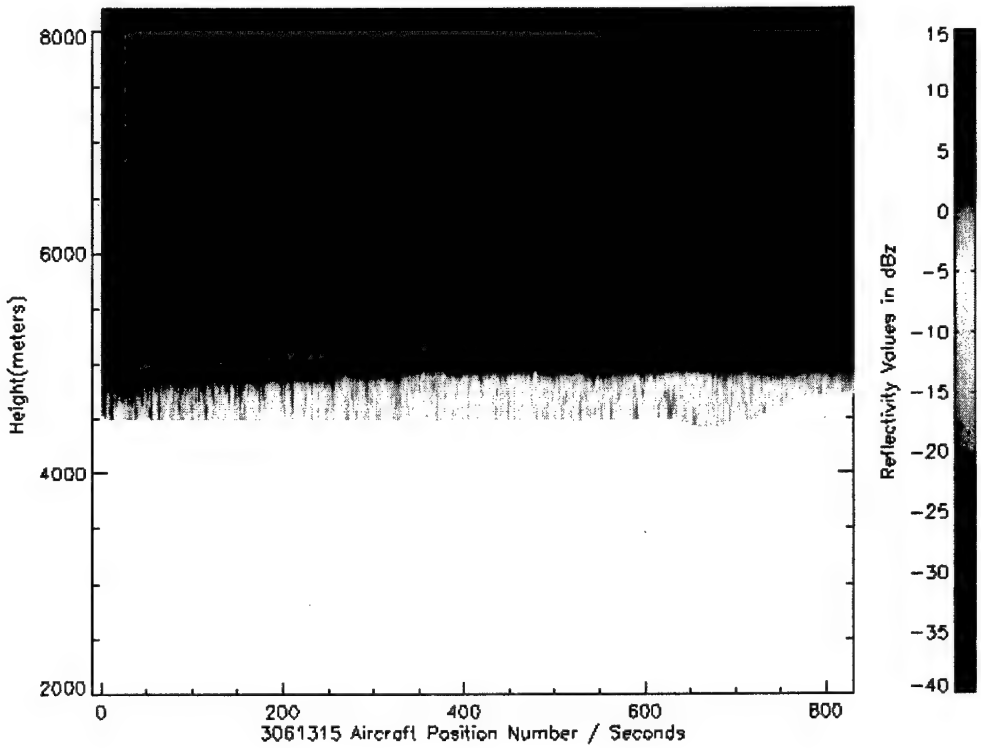

Figure 4.1. Radar Reflectivity showing cloud top height

A histogram of the approximately 130,000 reflectivity samples was plotted in order to determine the threshold for the binary cloud mask. An example of a cloud mask histogram is shown in Fig 4.2.

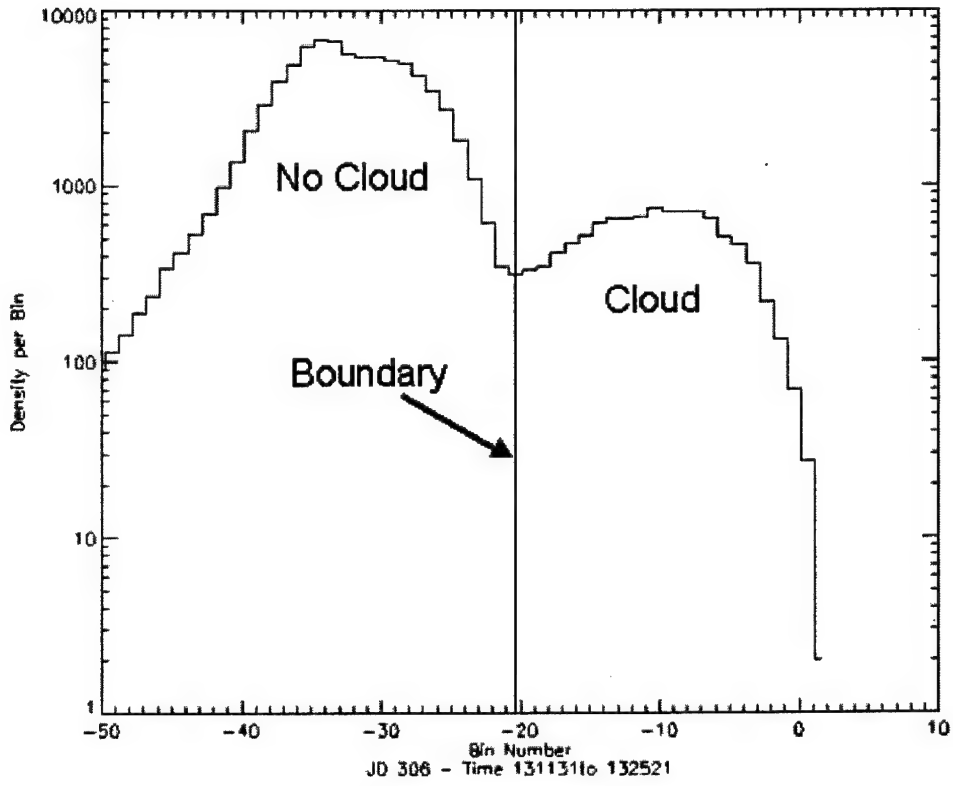

Figure 4.2 Histogram of Radar Reflectivity

The histogram was created using 1 dBz wide bins. *A log scale was used due to the large number of non-cloud filled range gates in the image.* The results of the histogram show two peaks of maximum occurrence, one near -35 dBz and one near -8 dBz. The most negative reflectivities are from the cloud-free range gates (i.e. no hydrometeors) and the larger valued reflectivities represent the cloud-filled range gates. The boundary drawn in the figure represents the point at which the method cannot distinguish between cloud-free and cloud-filled range gates and represents the cloud top. This value, near -20 dBz, was chosen as the threshold for this particular time frame.

Once the threshold was determined by the histogram method, the radar arrays were scanned and assigned their respective cloud mask values. Reflectivity values below the threshold were determined to be cloud-free and reflectivity values greater than the

threshold were determined to be cloud-filled. The array was then scanned from the first range gate to the last and the first range gate to appear cloud-free was assigned as the cloud top for each 1-second scan. Results of the threshold technique for the same time period shown in Fig 4.1 are shown in Figure 4.3.

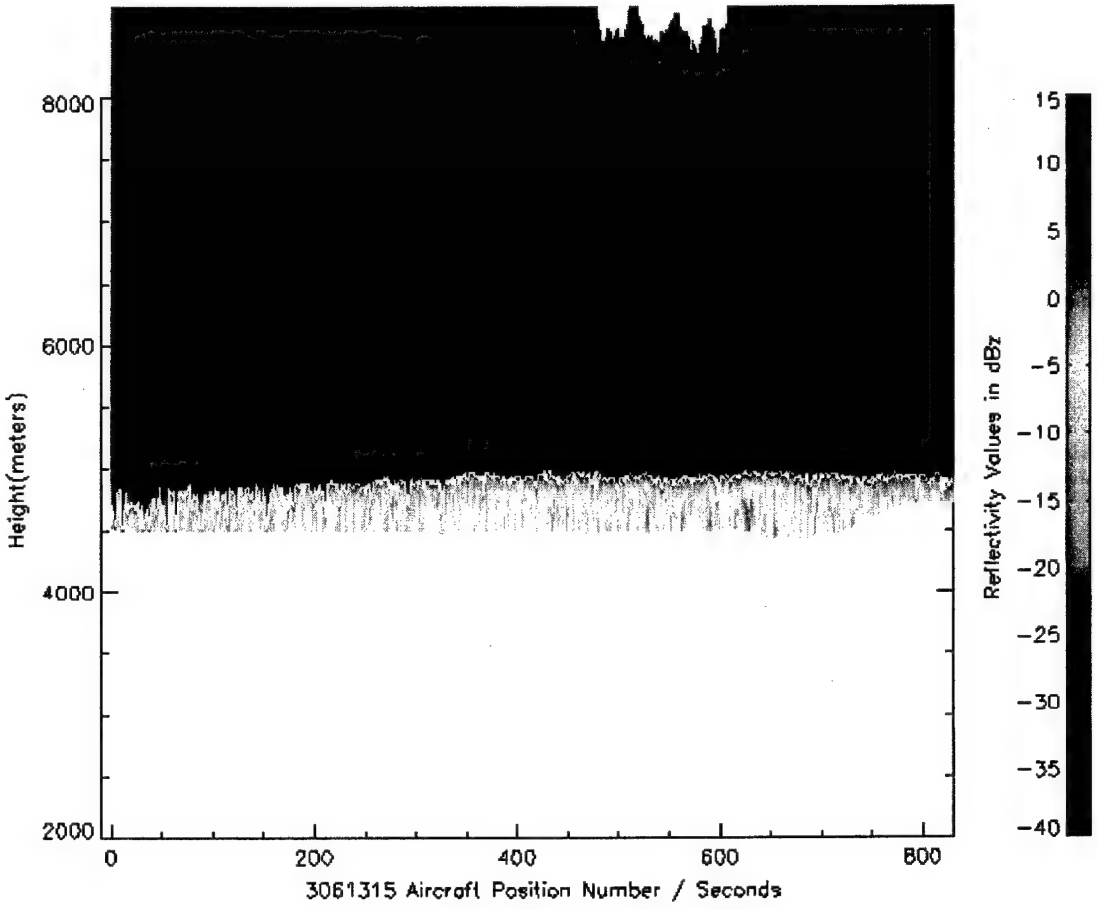

Figure 4.3. Results of Radar Cloud Height Algorithm (Cloud top = bright white)

For the 2 Nov case, the threshold used was -20 dBz. However, occasionally the 14 Oct case showed a less sensitive threshold. Fig 4.4 shows a cloud mask histogram which shows a less sensitive threshold of approximately -15 dBz.

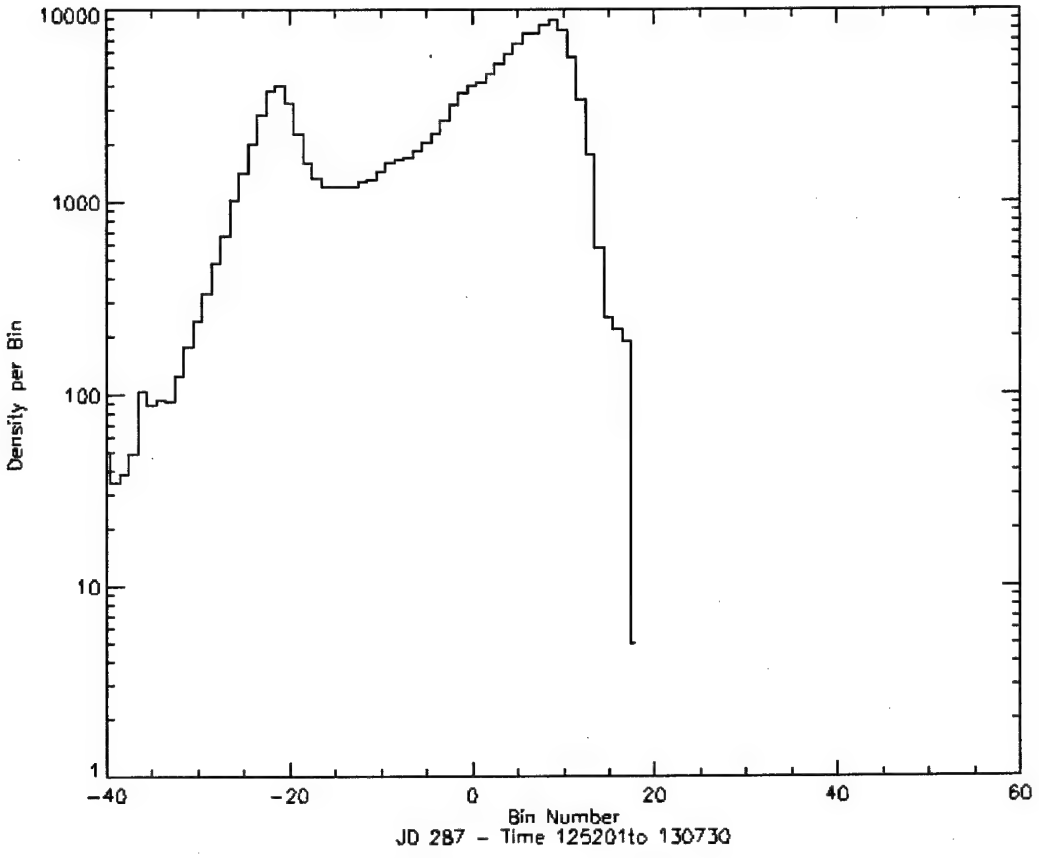

Figure 4.4. Histogram of radar Reflectivity – 14 Oct 01

This can be explained by attenuation problems associated with 95GHz radars. The aircraft was flying within 500 m of the cloud top on 2 Nov (see Fig 4.1) and at times during 14 Oct as much as 3.5 km below cloud top while sampling thick clouds. Fig. 4.5 shows the reflectivity image and radar derived cloud top in white.

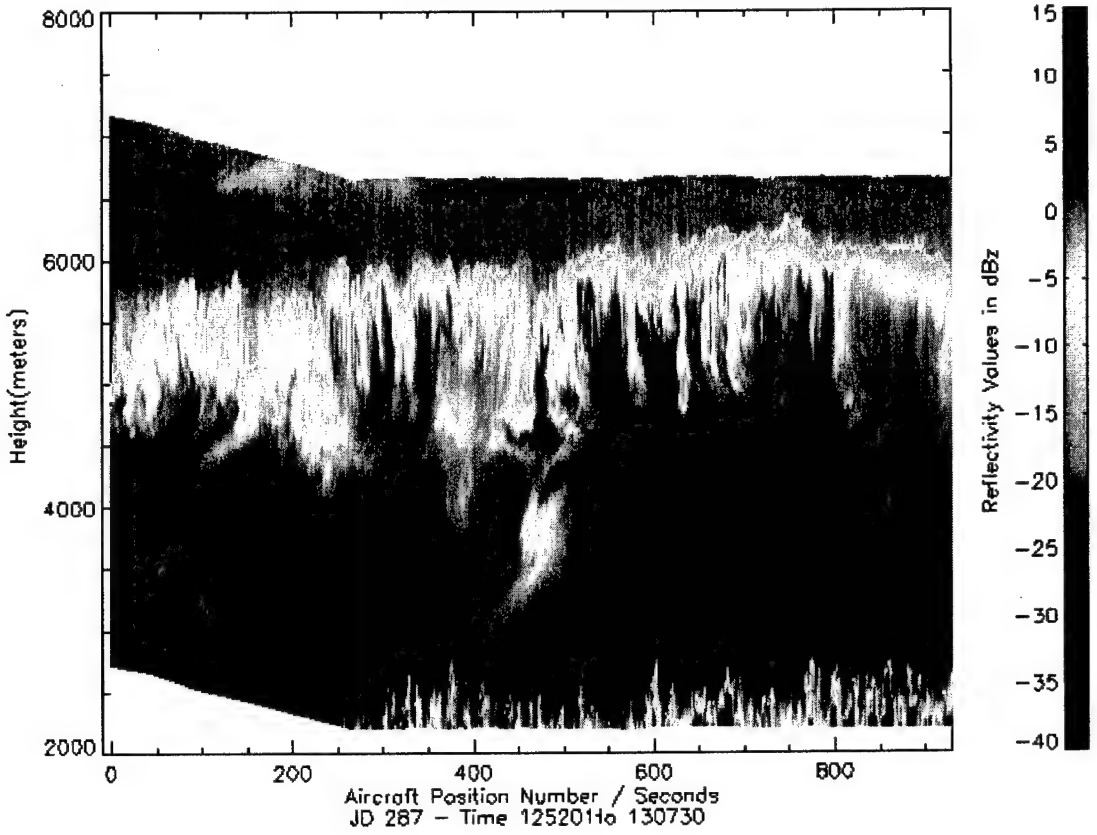

Figure 4.5. Radar Reflectivity and Radar Cloud Top – 14 Oct 01

The threshold ranged from –15 dBz to –23 dBz due to the wider variety of sampling strategies used on 14 Oct. These results are comparable to the results for cloud boundaries determined by radar in Paluch et al. (1996). Cloud edges in that case showed reflectivities in the range of -15 dBz to -20 dBz.

Since the radar data was considered the most accurate measure of the exact position of the cloud, it was used as the "ground truth" in this study. However, determining the exact height of the cloud top by radar is not exact. There is some error in the determination of cloud top height. The greatest source of error in radar data comes not from the radar but from the GPS. The vertical height accuracy of the GPS is +/- 30

m. The next source of error comes from the smoothing of the data in 30 m range gates. Cloud top can occur at any point in a range gate, but would be assigned the mean height for the range gate by the algorithm. The mean reflectivity in a range gate is what the radar measures. So an abrupt cloud top in a range gate results some smoothing in the data. A good error estimate for this type of error is 15 m, one half of a range gate. The thresholding technique also has some error in determining the cloud top height but seldom more than one range gate. The total maximum error for radar cloud top measurements used for the remainder of this study is +/- 75 m which is more than adequate for the comparisons with satellite data.

4.2. Satellite Derived Cloud Heights – Black Body Method

This method is the most common used to convert satellite-measured radiances to cloud top height. The process starts with the Planck function:

$$B_\lambda(T) = \frac{2hc^2\lambda^{-5}}{\exp(\frac{hc}{\lambda kT}) - 1}$$

By inverting the Planck function, one can solve the equation for brightness temperature (T_b) to get:

$$T_b = \frac{hc}{\lambda k \ln[(\frac{2hc^2\lambda^{-5}}{B_\lambda(T)}) + 1]}$$

This temperature represents the environmental temperature at which particles radiate if the assumption is made that the cloud is a black body (emissivity (ε) = 1). When a comparison is made with a sounding in the vicinity of the particles in question, a height

can be determined using a linear interpolation of temperature versus height. Fig. 4.6 shows an infrared (IR) image from the 2 Nov case.

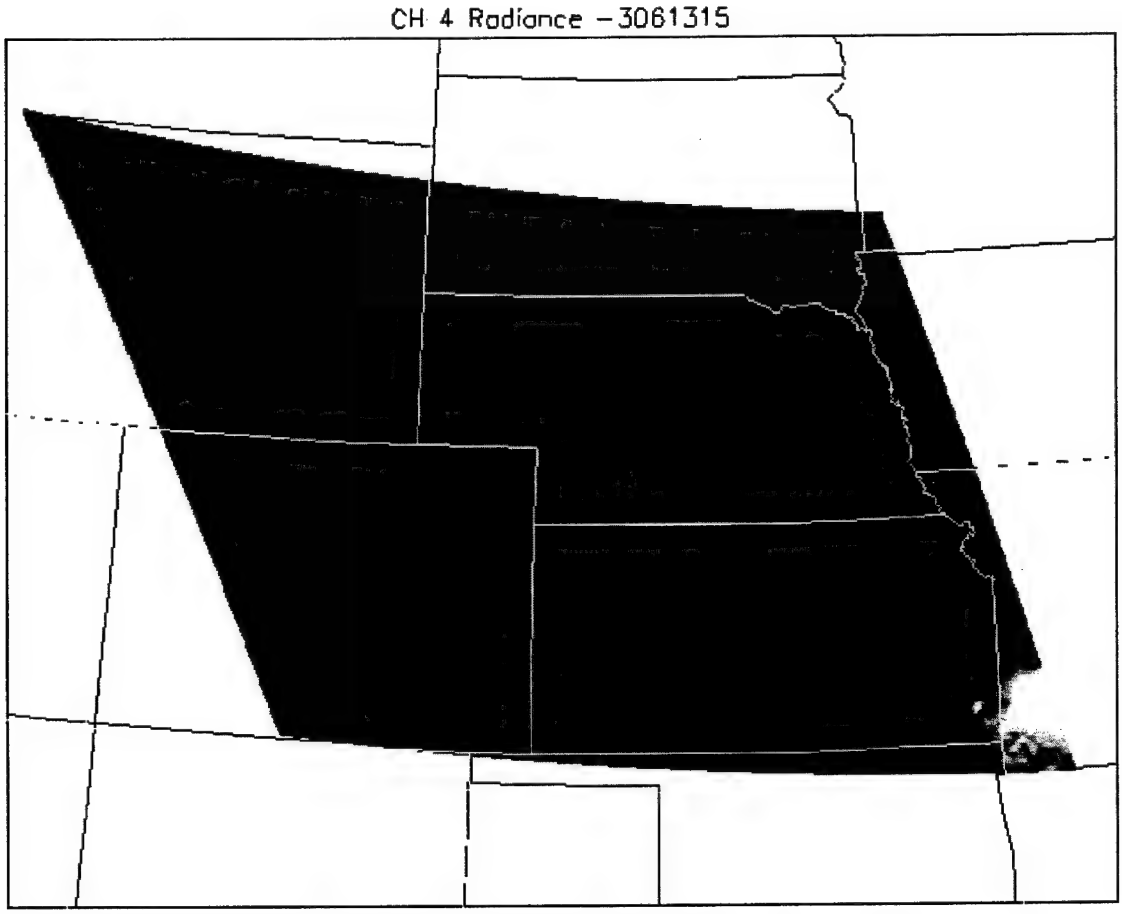

Figure 4.6. IR Image with Flight Path of WKA (black line)

The radiance values were converted to height, then the radar and satellite derived heights were matched along the flight path and compared (Fig 4.7).

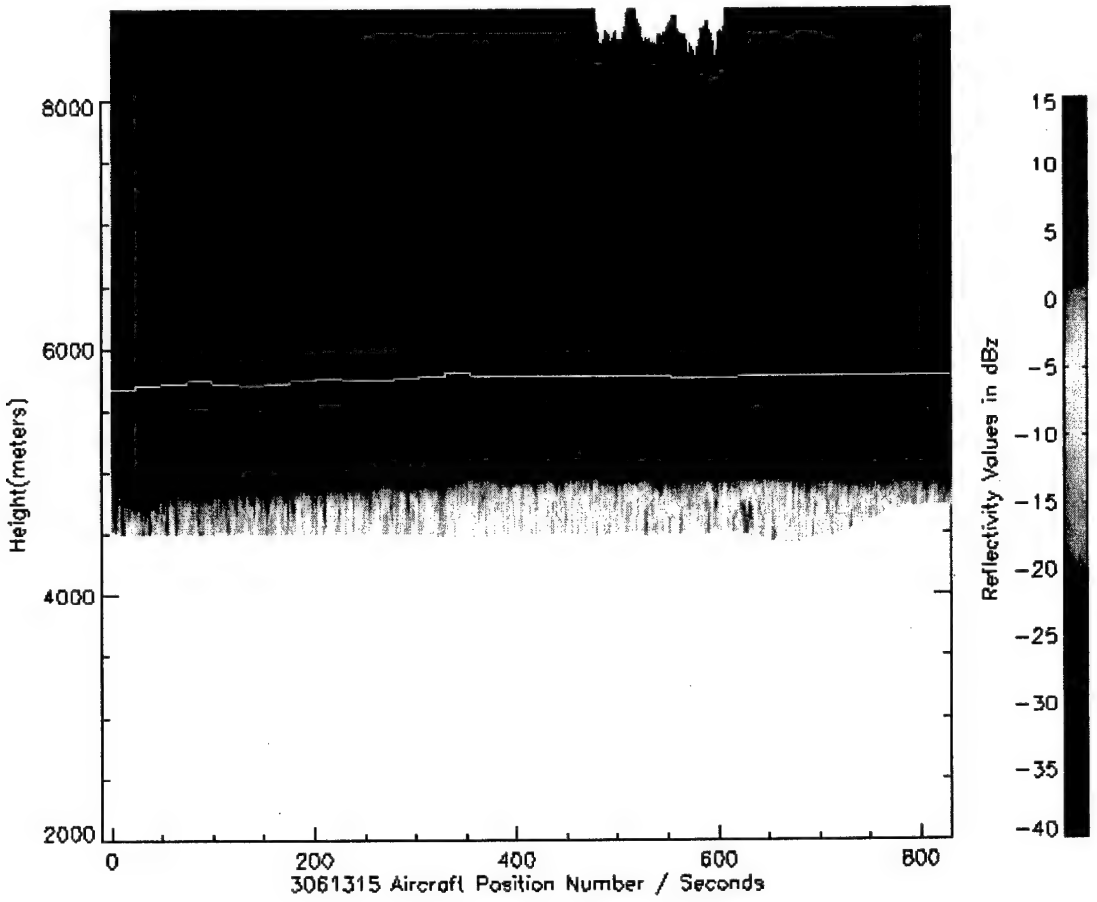

Figure 4.7. Black Body Heights Compared to Radar (BB Height –white line)

The most noticeable feature in this comparison is the difference in the satellite-derived cloud top versus the radar-derived cloud top. Fig 4.8 shows a comparison between the two methods of cloud top height determination and the difference.

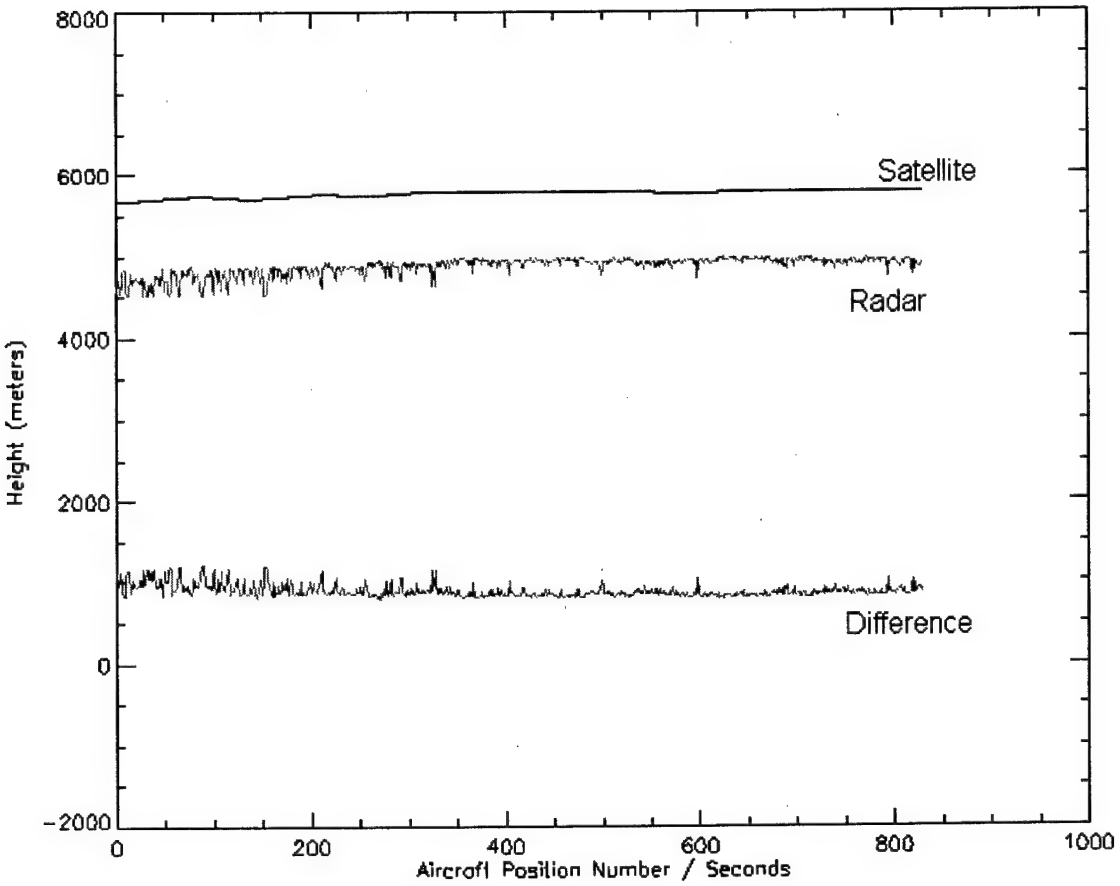

Figure 4.8. Comparison of Radar and Black Body Derived Cloud Top Heights

The satellite-derived top has a bias of +890 m for this time period when compared to radar. One primary reason for this is attenuation by atmosphere above the cloud. One possible method for correction of this is described in Joyce (2000). The amount of correction is a function of the radiance, satellite zenith angle, latitude and season. Fig 4.9 shows the result of this correction.

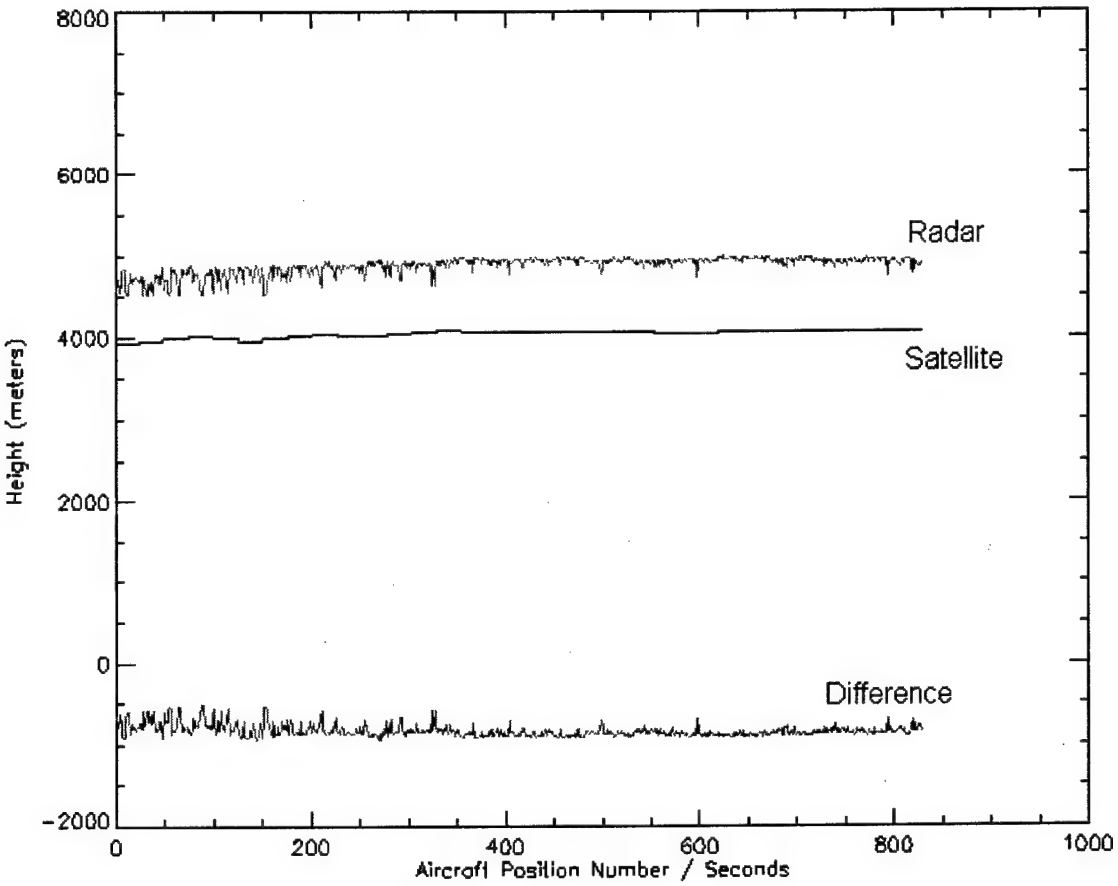

Figure 4.9. Corrected Satellite Derived Cloud Tops Compared to Radar

After the correction, the bias was reduced in magnitude to 840 m, but the satellite-derived cloud top was lower than the radar top. This is expected in the case of optically thin clouds as the radiation from warmer regions below the cloud contaminates the FOV as seen from the satellite.

When clouds become extremely thin the black body method has greater difficulty determining cloud top height. That point is illustrated in the 2 Nov case at 1615Z. Fig 4.10 shows the infrared image with the region sampled by aircraft.

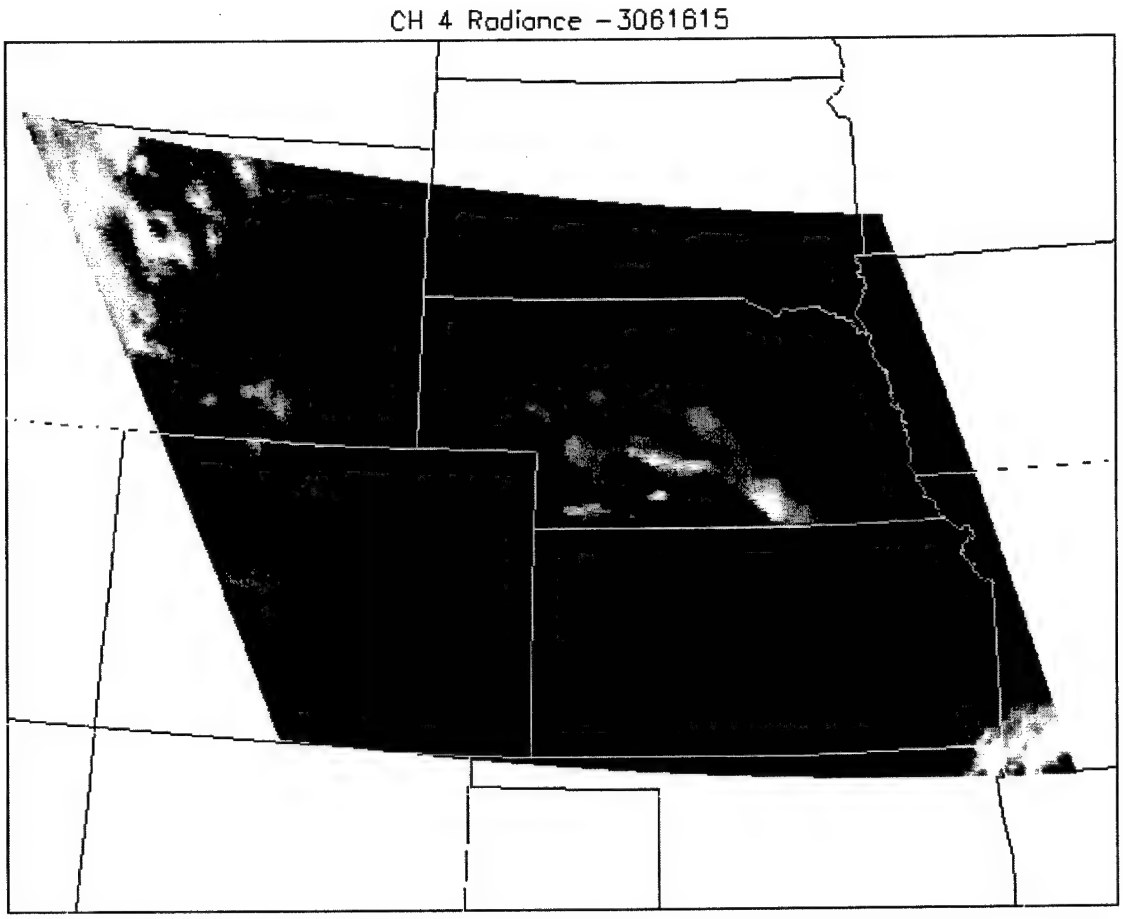

Figure 4.10. IR Image with Flight Path of WKA (black line) - 1615Z

At this time the cloud had begun to dissipate and only lasted for about another hour. The aircraft sampled an extremely thin portion of the cloud. The black body comparison to radar is shown in Fig. 4.11.

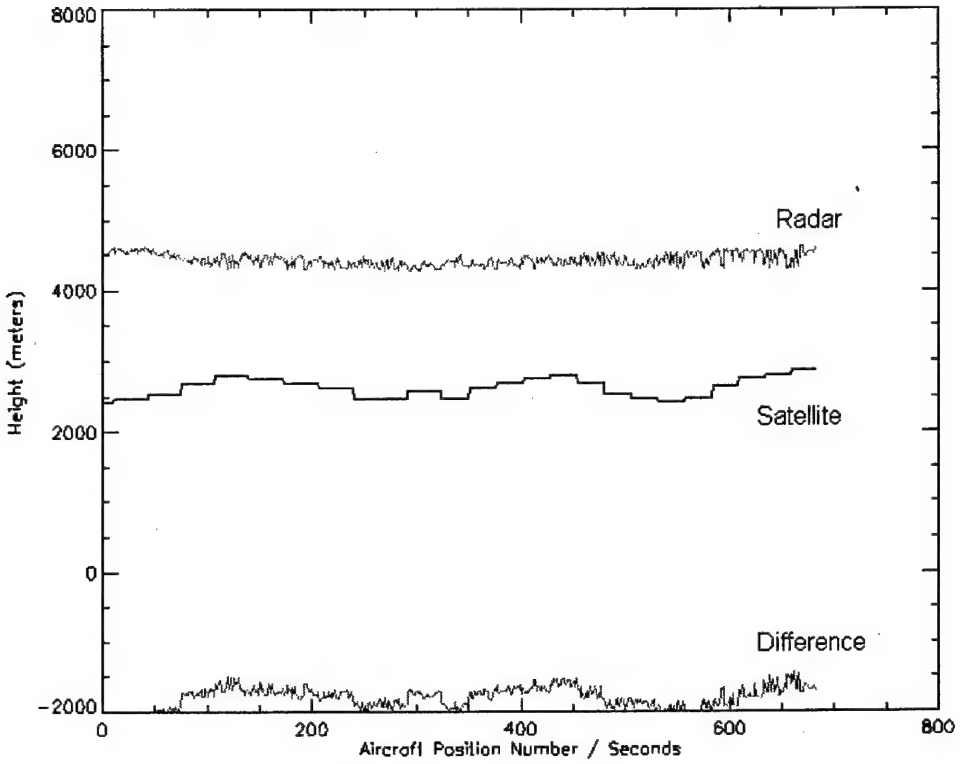

Figure 4.11. Comparison of Radar and Black Body Derived Cloud Top

The bias in this case is greater than 1800 m below the radar measured cloud top. This result is due to the low emissivity of the clouds and partially filled FOVs. If accurate height determination of optically thin clouds is desired, a method that can detect partially-filled FOVs and account for non-black emissivities is needed. The next section describes the Spatial Coherence method, which can account for these difficulties.

4.3. Satellite Derived Cloud Heights – Spatial Coherence Method

The Spatial Coherence method was developed to determine cloud cover and clear sky radiances (Coakley and Bretherton,1982). However, the method can also be used to determine a mean cloud top radiance in some circumstances. When a simple cloud scene exists, spatial coherence can produce a mean cloud top radiance, a mean surface radiance

and variability of both parameters. The cloud top radiance can be converted to a brightness temperature and a cloud top height when compared to a sounding. In addition to surface and cloud top radiances, spatial coherence can be used to determine the amount and the emissivity of cloud in each FOV in a scene. This technique gives information about partially filled FOVs or areas where the cloud is optically thin. Knowledge of these properties gives an idea of accuracy of height determinations and can lead to additional methods to determine cloud top.

The method starts by determining a cloud scene. The scene must be limited in horizontal scale and works best when only one cloud layer exists in the scene. The scene must contain areas of clear sky and cloudy FOVs. Fig 4.12 shows an example of a cloud scene. The scene chosen is shown in inverse gray scale.

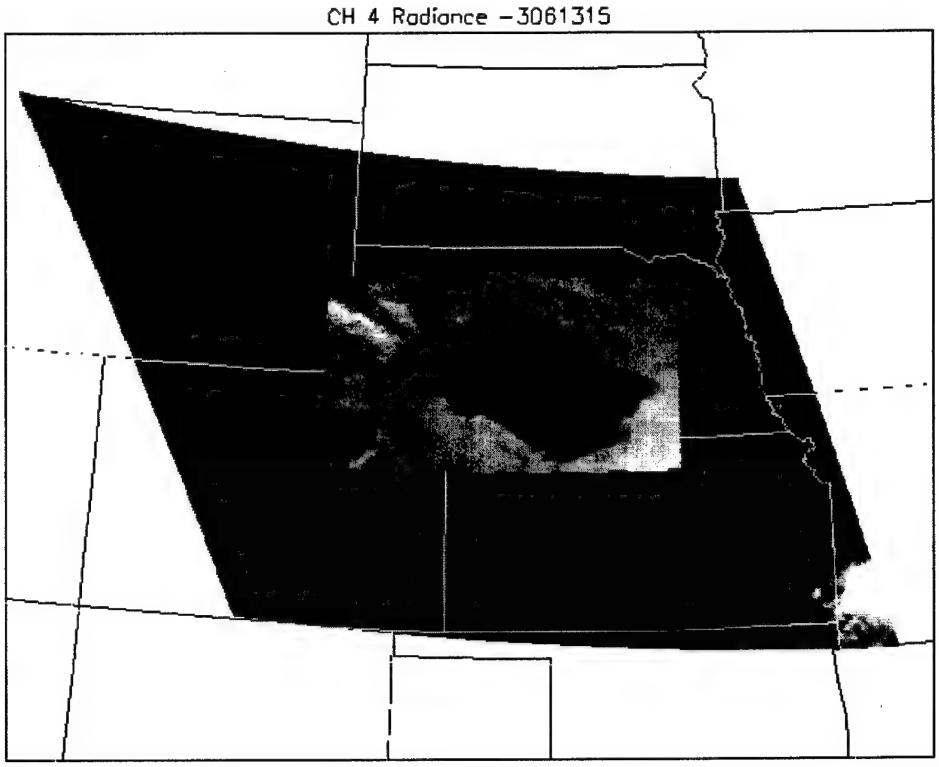

Figure 4.12. Channel 4 radiance with Cloud Scene (inverse gray scale)

Each FOV in the selected scene is then scrutinized individually by taking it and the eight surrounding FOVs and calculating the mean and standard deviation for each grouping. The results for each scene are plotted on a scatter plot with the mean as the ordinate and the standard deviation as the abscissa. A well-behaved cloud scene produces an arch with clusters of points with minimal standard deviation. These clusters, or "feet of the arch", indicate the mean value of cloud top radiance and clear FOV radiance, i.e. surface radiance. Fig 4.13 shows an example of this type of plot.

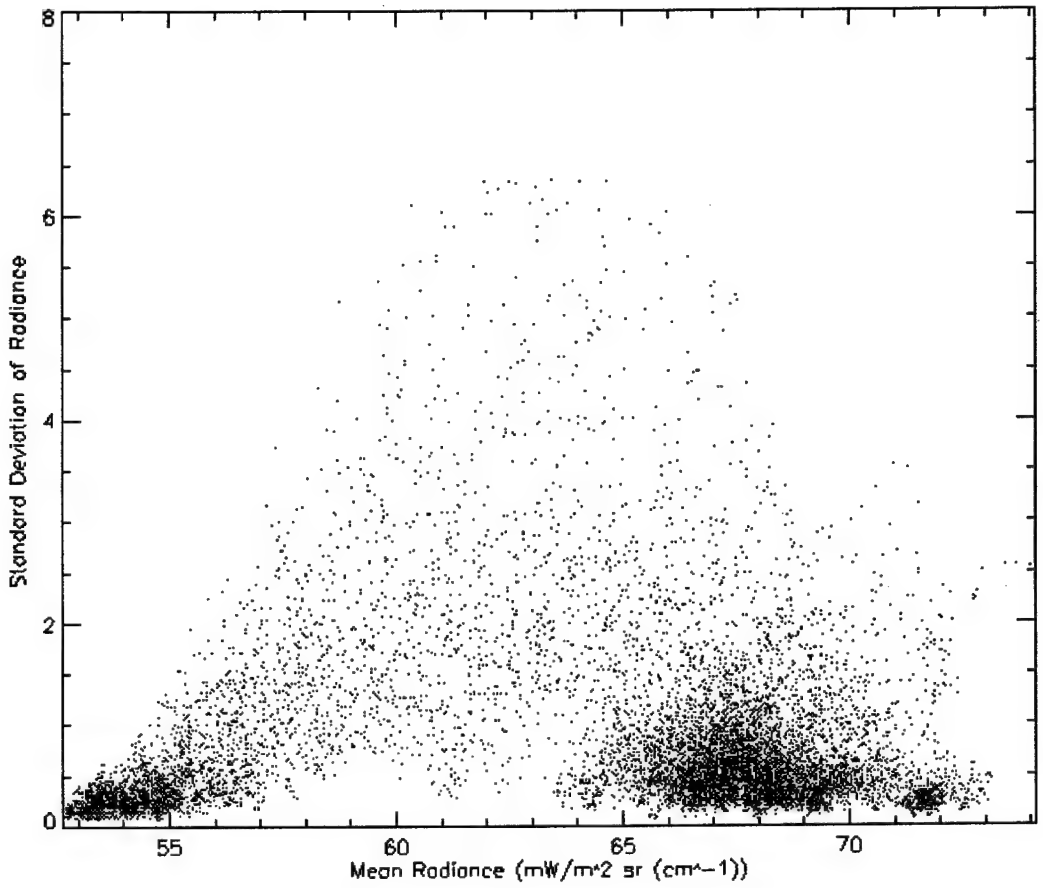

Figure 4.13. Spatial Coherence Scatter Plot for 2 Nov 01 – 1315Z

The mean cloud top radiance (L_{cld}) from this example would be ~ 54 mW/[m^2 sr cm^{-1}] and the mean surface radiance (L_{clr}) would be ~ 68 mW/[m^2 sr cm^{-1}]. Additionally, the width of the feet determine the variability in the measurements. This can be useful in determining the accuracy of the height retrieval.

Once a value of L_{cld} is chosen, a mean cloud top for the scene can be calculated using the Planck function and a sounding in a similar manner as the black body method. The underlying assumption when using this method to determine cloud top is that the value of L_{cld} becomes the black body radiance of the cloud top. Fig 4.14 shows the results of this method compared to radar.

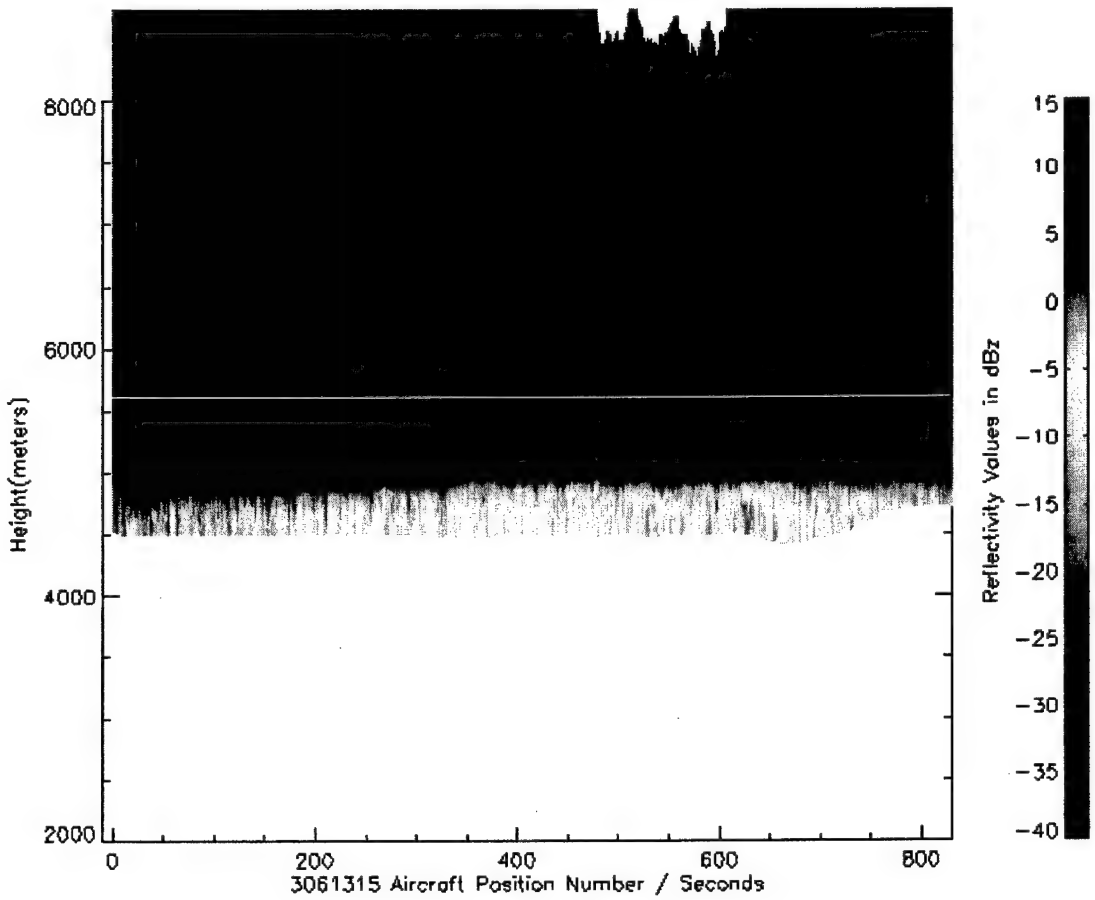

Figure 4.14. Spatial Coherence Heights Compared to Radar (SC Height –white line)

As in the black body method, the height of the spatial coherence method is higher than the radar cloud top. This makes sense because the radiances used to calculate the black body height were the same radiances used to calculate the spatial coherence heights. Also it is important to note that only one value of cloud top is calculated for the entire scene. This allows for no variability in the cloud top in a particular scene. This would limit this method's use to stratiform type clouds. Fig 4.15 shows a comparison between the spatial coherence and radar cloud top heights and the difference.

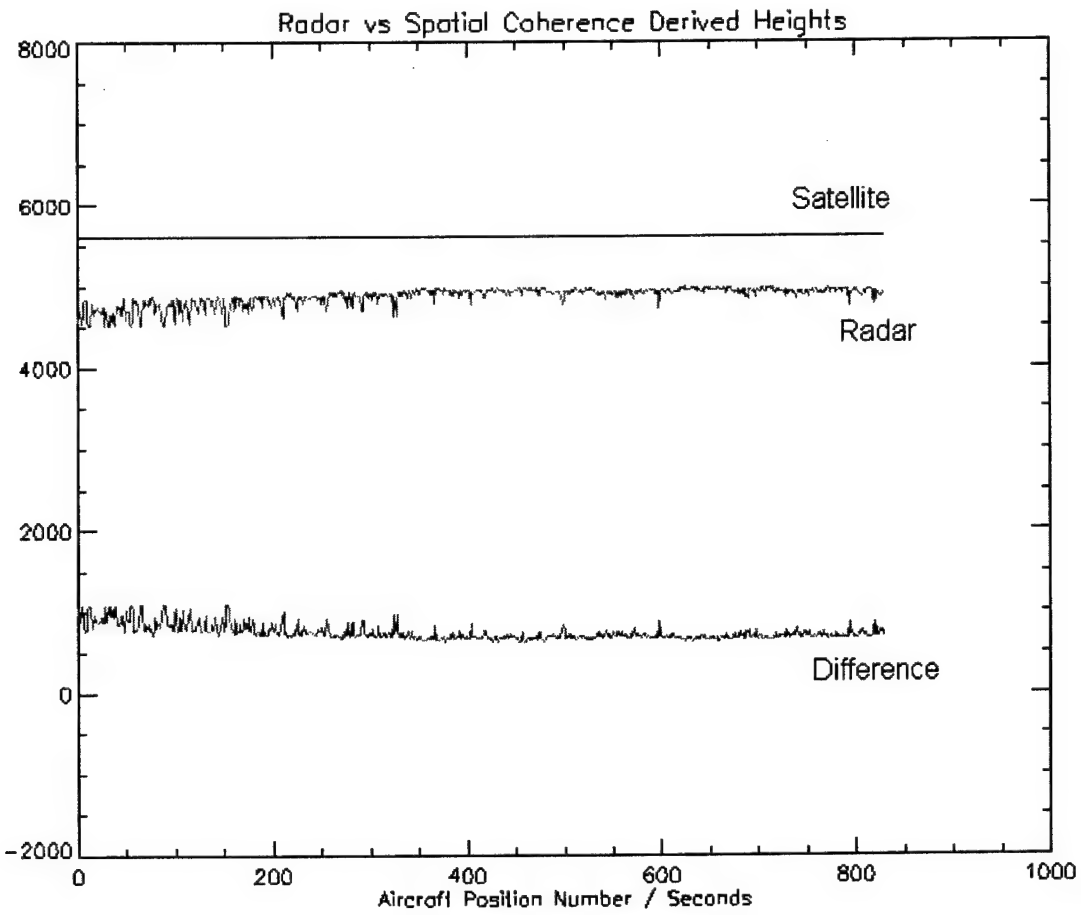

Figure 4.15. Comparison of Radar and Satellite Derived Cloud Top Heights

The spatial coherence cloud top has a bias of +750 m for this time period when compared to radar. As in the black body case, a primary reason for this is attenuation by the atmosphere above the cloud. When the zenith angle correction was applied the bias became negative (satellite top below radar top) as in the black body case.

Although there is still considerable error with the spatial coherence method, the real strength comes to light in the case of an optically thin cloud. When a cloud becomes extremely thin, the black body method fails miserably. As long as there is some portion of the cloud radiating at near black body temperatures, the spatial coherence method can detect the cloud reasonably close to the actual height. As previously discussed, the 2 Nov

case at 1615Z illustrates this. The spatial coherence comparison for this time is shown in Fig. 4.16.

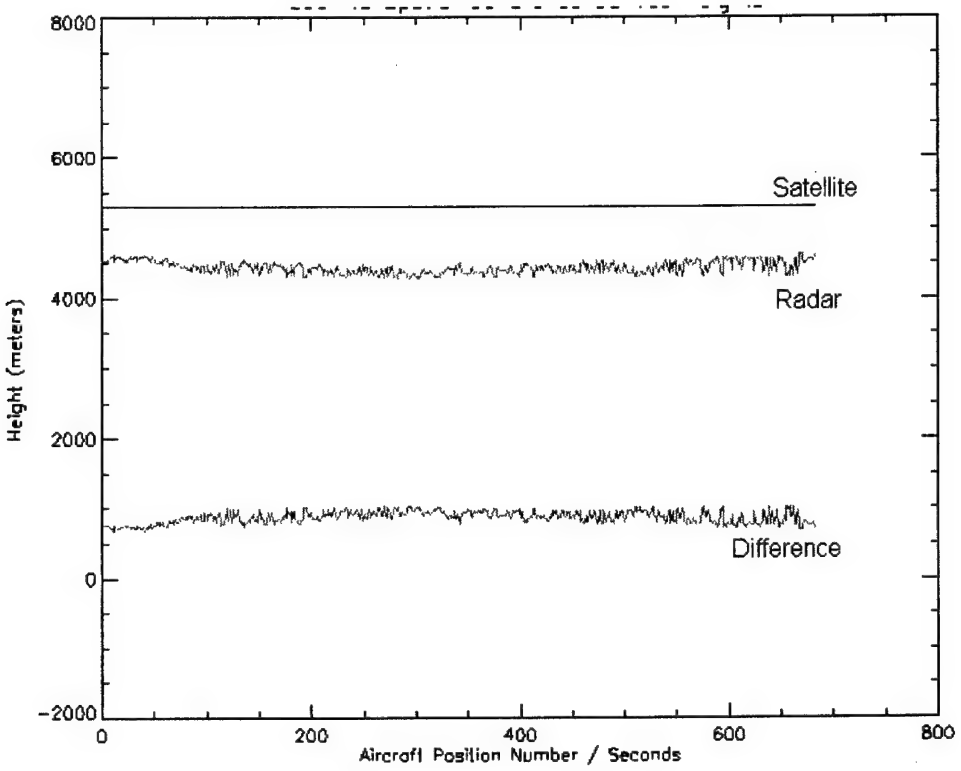

Figure 4.16. Comparison of Radar and Spatial Coherence Derived Cloud Top

The spatial coherence method produced a height biased 870 m above the radar. (Recall the 1800 m biased low from the black body method as shown in Fig 4.11.). In the case of an optically thin cloud, the spatial coherence method would be the preferential method to determine the height. However, the bias is still quite large for the spatial coherence method in all cases. This result still suggests a more accurate determination should be sought.

The spatial coherence method can be extended to learn more about the clouds within a particular scene. From the scatter plots similar to that shown in Fig 4.13, mean cloud top and surface radiances for the scene can be determined. Cloud amount and

emissivity, the product of which is called Effective Cloud Amount, can be calculated for each FOV as well. By using:

$$L_\lambda = (1 - N'_\lambda) L_{clr} + N'_\lambda L_{cld}$$

where L_λ represents the radiance measured at the satellite sensor; N'_λ, effective cloud amount and L_{clr} and L_{cld} represent the clear and cloud radiances respectively. Solving for N'_λ, yields:

$$N'_\lambda = \frac{L_\lambda - L_{clr(\lambda)}}{L_{cld(\lambda)} - L_{clr(\lambda)}}$$

This value can be used to assess the optical thickness of the cloud in a particular FOV and can be used to determine the best method to determine cloud top height or the accuracy of the height value. The next chapter introduces an optimal estimation method that uses an effective cloud amount threshold to determine the application of cloud top height determination schemes.

4.4. Satellite Derived Cloud Heights – Optimal Estimation Method

The optimal estimation method used in this study was derived from a method described in Rodgers (1990) and further explained in Engelen and Stephens(1997). It starts with a measurement y and a forward function, F(x), which describes some radiance value as a function of height, x, such that:

$$y = F(x) + \varepsilon$$

where ε represents the error in the measurement system. The measurement in this case is the 10.7 um radiance value (L_{ch4}). It is combined with the spatial coherence mean (L_{cld}) for cloudy FOVs in the scene. The two values were combined as independent measurements using the reciprocal of the square of the standard deviations as a weight:

$$y = \frac{L_{ch4}/\sigma_{ch4}^2 + L_{cld}/\sigma_{sc}^2}{1/\sigma_{ch4}^2 + 1/\sigma_{sc}^2}$$

The reason for this combination of measurements was to investigate a more accurate method to determine cloud top height of the optically thin portions of the cloud. The radiance measurements will be biased low when the cloud becomes optically thin, whereas the spatial coherence mean will remain constant for a particular scene regardless of the optical thickness of a particular FOV. The variances for each measurement were determined by the results of cloud top comparisons of the two methods to radar data. It is important to note that this combination of measurements was only performed in FOVs that exceeded a threshold value of N'.

The N' threshold was determined by a similar histogram technique used in the radar cloud mask algorithm. Once N' values were calculated for all FOVs in a cloud scene, the results were histogramed and plotted. Fig 4.17 shows an example of the histogram technique for 2 Nov 1315Z.

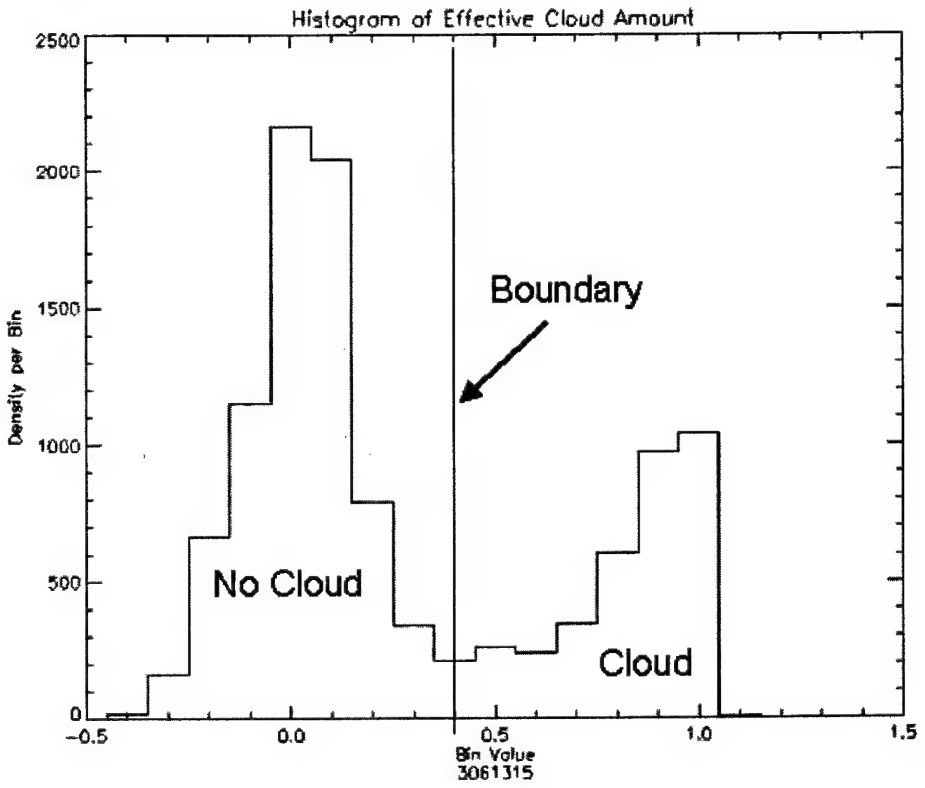

Figure 4.17. Histogram of Effective Cloud Amount

The resulting histogram shows two peaks. The largest peak, centered on N' = 0, represents the FOVs with very little to no cloud filling the FOV. The second peak, maximized on N' = 1, represents the mostly cloud-filled FOVs. The boundary where the two peaks intersect represents the N' threshold between cloud and non-cloud filled FOVs. This threshold was generally about .4, which represented a FOV with at least 4/10 cloud coverage or greater. This result was noted in almost all cases.

In the optimal estimation algorithm, when a FOV contained less than 4/10 cloud coverage, i.e. N' less than .4, the routine returned a 'not retrievable' flag. In this case, the Ch 4 radiance value represents the surface radiance (or moist layers close to the surface) and no height retrieval was meaningful. The thresholding method produced good results

in cloud top height at the edges of clouds, without falsely modifying surface radiances by averaging them with the spatial coherence mean.

The forward function, F(x), used in this method was a two-step process consisting of a linear interpolation of height to temperature and then converting the value to a radiance with the Planck function. The conversion from height to temperature was performed using a typical mid-latitude, summer sounding that had been adjusted to match a local sounding. The lapse rates of the typical sounding and the local sounding were similar (see Appendix B). This typical sounding was free from inversions that can cause difficulties in proper vertical placement of clouds. After converting height to a temperature, the GVAR Planck function was used to convert the temperature to a brightness temperature and finally radiance.

An initial value of cloud top height is necessary to start the algorithm. This a priori value, x_a, was chosen from the sounding near the cloud under scrutiny. The cloud layers were chosen from the height of the temperature and dew point fields where clouds seemed apparent. The variance of this height was made sufficiently large to account for spatial and temporal variations during the day.

With all these elements in place, the algorithm was started for the cloud scene. The weighting function, which is defined as $K = \partial F / \partial x$, was calculated using a simple perturbation method:

$$K = \frac{\mathrm{F}(1.01\hat{x}) - \mathrm{F}(0.99\hat{x})}{0.02\hat{x}}$$

Then a new value of x was calculated using:

$$x^{i+1} = \frac{S_a^{-1}x_a + KS_y^{-1}(y - F(x^i) + Kx^i)}{S_a^{-1} + K^2 S_y^{-1}}$$

and the error covariance of the current value of x was found using:

$$S_x^{-1} = S_a^{-1} + K^2 S_y^{-1}$$

The algorithm repeated until a convergence criterion was met. The convergence test used was:

$$\frac{(x^{i+1} - x^i)^2}{S_x} < .01$$

Once the convergence criterion was met, the value of the height was assigned to the FOV. The A parameter and χ^2 were calculated for each FOV as well. The A parameter was calculated using:

$$A = 1 - \frac{1}{1 + K^2 \frac{S_a}{S_y}}$$

The A parameter was used to diagnose the dependence of the retrieval on the specified a priori cloud top height. Too great of a reliance on the a priori would defeat the purpose of remote sensing in this case. The a priori estimate was given a large variance to ensure a heavy reliance on the measurement.

χ^2 was found by using:

$$\chi^2 = \frac{(y - F(x^i))^2}{S_y} + \frac{(x_a - x_i)^2}{S_a}$$

This formulation of χ^2 allows for one degree of freedom. Using this, a moderately good retrieval would have $\chi^2 \sim 1$ according to Engelen and Stephens (1997).

This process was repeated for all the FOVs in the scene. The result was an array of cloud top heights. FOV to aircraft position collocation was performed as described in

Chapter 3 and the results were compared to radar-estimated heights. Fig 4.18 shows the results for the 2 Nov, 1315Z case.

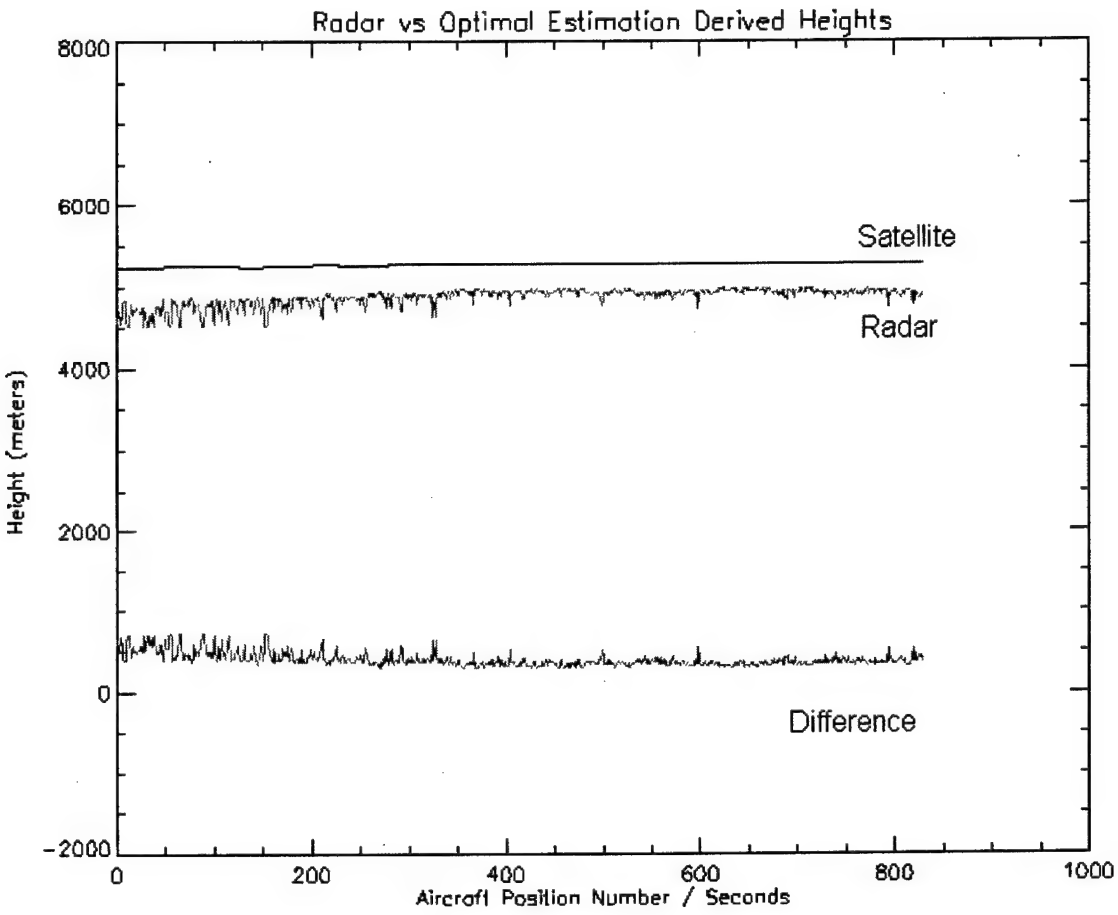

Figure 4.18. Comparison of Radar and OE Derived Cloud Top –1315Z

The bias for this time was ~ +400 m. This is an improvement over the two previous methods. One reason is the use of the climatological sounding instead of the actual sounding for conversion of temperature to height. Actual soundings contain inversions and isothermal layers that can lead to uncertainty in the linear interpolation of temperature to height. The ideal sounding, based on climatology, used in the optimal estimation method contained neither of these. While this is a slight improvement over the two previous methods, the most impressive results come from the previously

discussed, optically-thin timeframe around 1615Z. The results for that time are shown in Fig. 4.19.

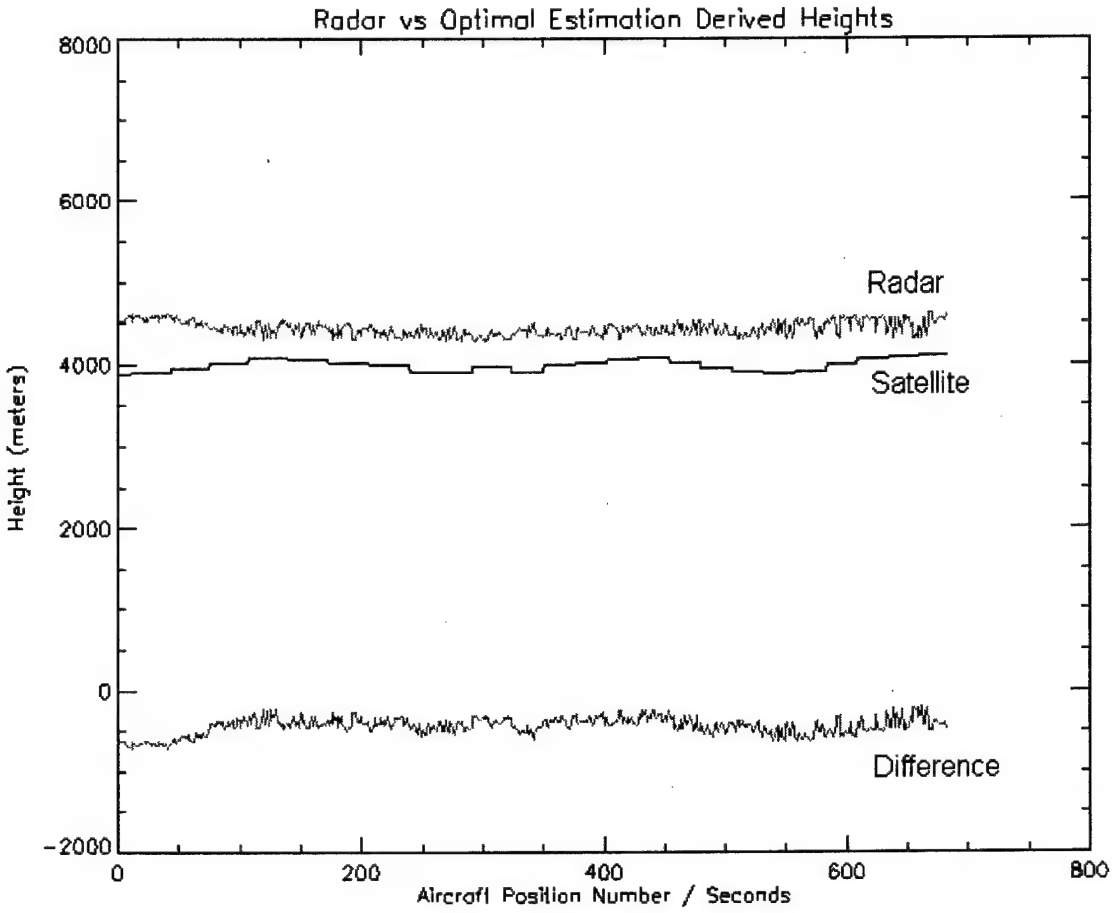

Figure 4.19. Comparison of Radar and OE Derived Cloud Top – 1615Z

The bias for this time frame was 450 m below the radar measured cloud top. This is a large improvement over the two previous methods. The reason for the improvement over the black body method is the use of the spatial coherence to assist the retrieval in cloud top determination when optically thin clouds are present in the FOV. The reason for the improvement over the spatial coherence method is the use of the ideal sounding as previously discussed.

Optimal Estimation routines also come with diagnostics to describe the details of the retrieval. The A parameter describes the weighting of the a priori estimate and its influence on the retrieval.

The A parameter for the 1315Z retrieval was ~ .96 indicating a strong reliance on the measurement. This parameter is tunable by adjusting the a priori variance. Decreasing the variance would force the algorithm to rely on the a priori estimate more strongly and the result would be a height retrieval closer to the a priori value and indicated by an A parameter closer to 0.

χ^2 values were also calculated for each of the height retrievals. The value of χ^2 should be close to 1 to indicate a good retrieval. Fig 4.20 shows the χ^2 values for the current case.

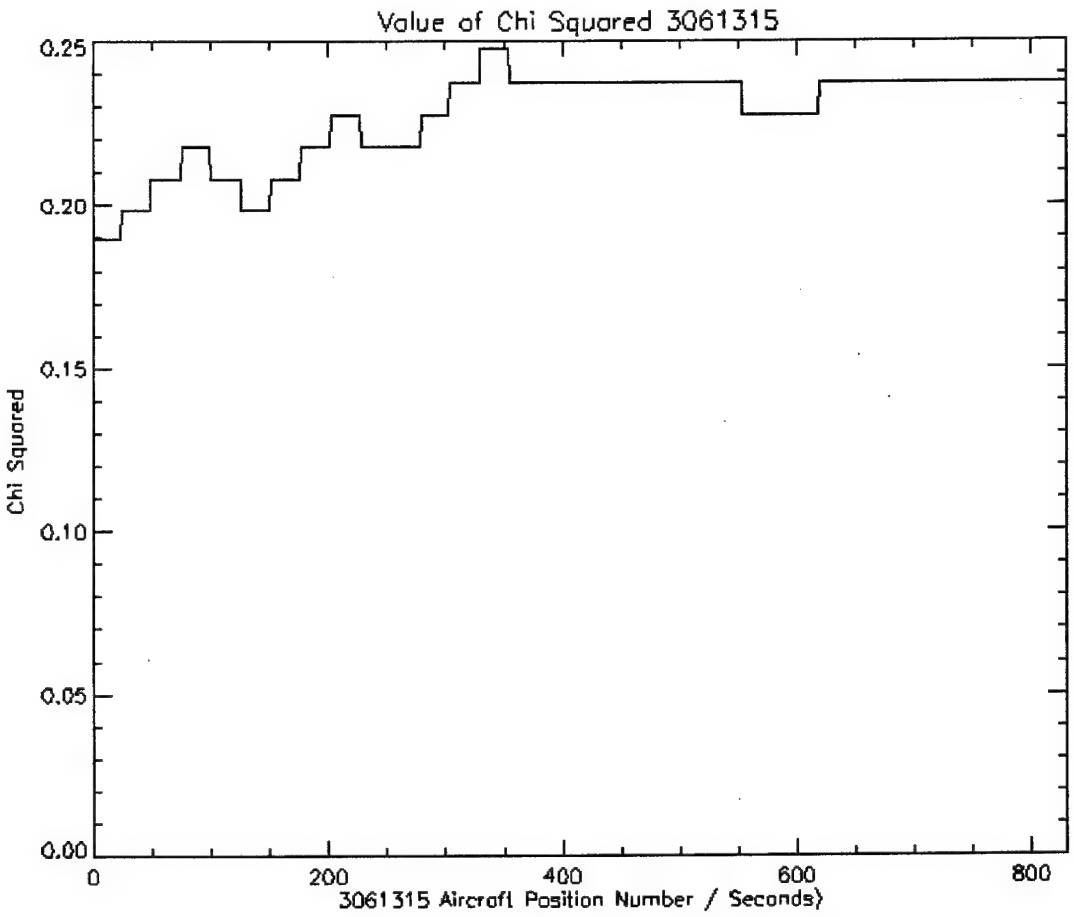

Figure 4.20. χ^2 values for 2 Nov 01 1315 Z

The χ^2 values are all much smaller than 1 indicating a good retrieval. In general, throughout the times on 2 Nov the χ^2 values were always less than 1 showing the optimal estimation method worked very well for this particular day and type of cloud.

The Error Covariance (Sx) for the retrievals was also calculated. Fig. 4.21 shows the error covariance results.

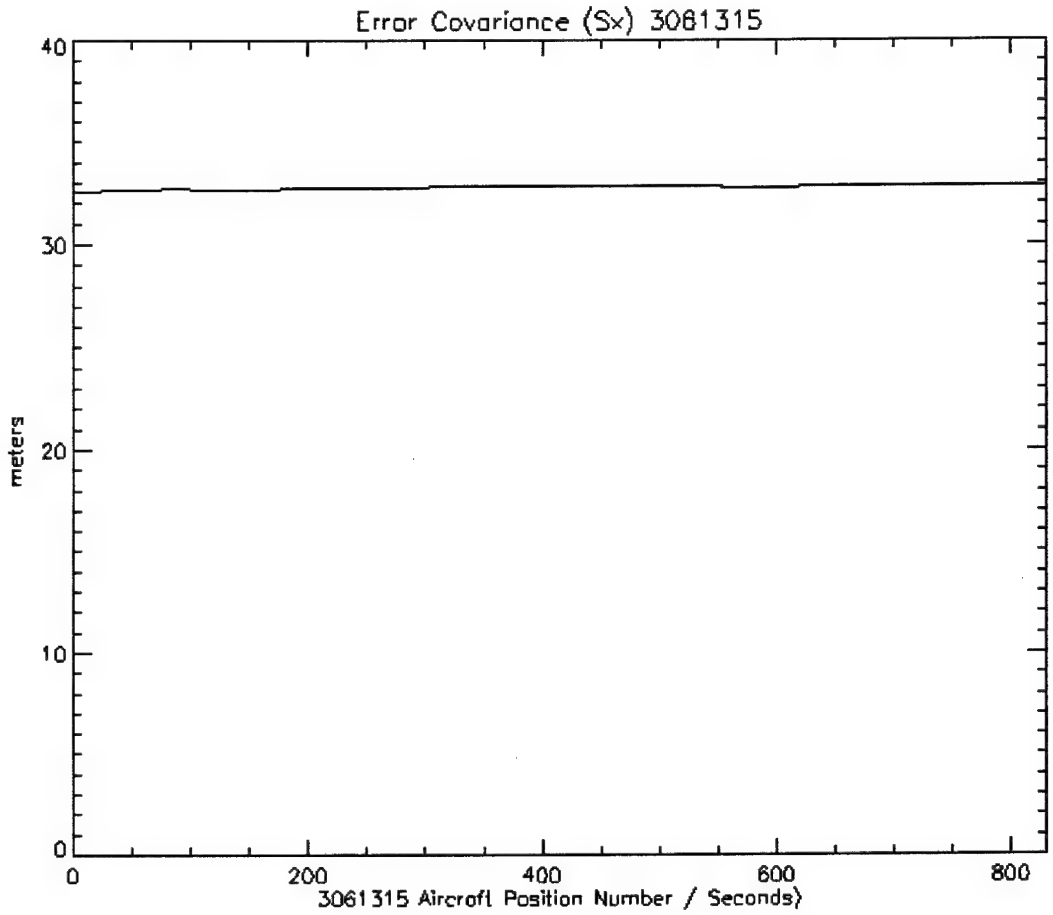

Figure 4.21. Error Covariance for 2 Nov 1315Z

The error covariance shows the accuracy of the retrieval. The value of Sx was approximately 32 meters throughout the 2 Nov case.

CHAPTER 5 – SUMMARY OF COMPARISONS

In Chapter 4, results for specific times of day were given as examples during the description of the methodology. Rather than describe each individual time frame of the two day time period, this chapter will summarize the results and make comparisons to similar work.

5.1. Black Body Method vs. Radar

During the 2 Nov case, a mid-level, mixed-phase cloud moved into the CLEX target region early in the morning (1200Z) and dissipated shortly after sunrise (~1615Z). The cloud top was well sampled by the vertical pointing radar throughout the lifecycle of the cloud. The cloud was first sampled in areas that appeared optically thick in the 10.7 um region and later in the life cycle areas that were optically thin. This provided an ideal data set to make cloud top comparisons.

Cloud tops, as measured by radar, ranged from 4500 m to 5000 m during this time. The cloud top radar threshold used was -20 dBz throughout the entire day. The black body method yielded cloud tops at approximately 5700 m to as low as 2000 m late in the period. Initial black body cloud tops were higher than the radar estimates. This error had many sources. A principle error source was the inversion present in the North Platte sounding. This cloud formed in a stable layer at ~ 4800 m. The inversion present in the sounding provided for numerous solutions to the brightness temperature to height

conversions. Another source of error was the possibility of a layer of undetectable thin cirrus above the cloud sampled by radar. The layer could have been beyond the range of the radar and too thin to provide a strong IR signature. However some cooling may have occurred if indeed the layer was there. These are all problems that cannot be accounted for with this method objectively. Later in the morning the black body cloud tops were below those measured by the radar. This was due to the thinning of the cloud as it dissipated. Since the cloud was not black (emissivity < 1), the surface radiance below the cloud biased the IR temperatures warmer resulting in a lower cloud top. With no way to determine the cloud amount or emmisivity, this problem cannot be corrected by this method alone. The biases for this method ranged from +900 m in optically thick FOVs to -2500 m for optically thin FOVs. These results are similar to those documented by Wylie (1989). Errors in thin cirrus, which share many of the same properties as CLEX clouds, using a CO_2 slicing technique compared to lidar measurements ranged from 50 mb to 100 mb. This translates to 700 m to 1200 m at pressures near 500 mb.

The zenith angle correction developed by Joyce (2001) seemed to overcorrect the heights for these types of clouds. With the corrections applied, errors ranged from –800 m to –3300 m. The zenith angle correction was intended for use in very opaque clouds (high emissivities). The clouds in CLEX are generally tenuous and small in scale with many partially filled FOVs which could lead to overcorrection.

Similarly, during the 14 Oct case, a mid-level, mixed-phase cloud moved into the CLEX target region early in the morning (1200Z). However, it did not dissipate after sunrise. Instead, the cloud persisted well into the afternoon until out of the CLEX target region. The cloud appeared slightly convective early in the period, evidenced by the

highly variable cloud top, but smoothed out to a more stratiform type by later in the day. The cloud top was well sampled by the vertical pointing radar throughout the time the cloud was in the target region. The cloud was sampled in areas that appeared optically thick in the 10.7 um region as well as optically thin areas. Numerous spiral descents through the cloud were made giving insight to the physical thickness of the cloud. This also provided an ideal data set to make cloud top comparisons with a more thorough understanding of the cloud.

Cloud tops, as measured by radar, were higher than the 2 Nov case and ranged from 5000 m to 5500 m. The cloud top radar threshold varied more due to the sampling technique of spiral descents and ascents through the cloud. This technique provided a trade off between a very sensitive radar cloud top measurement and a less sensitive but more revealing measurement of cloud thickness (cloud base and cloud top). The cloud sampled on this day was approximately 3000 m thick. The radar threshold varied from -13 dBz to –23 dBz. The black body method yielded cloud tops in the range of approximately 5500 m to 6000 m in optically thick areas of the cloud. As in the 2 Nov case the black body derived cloud tops were higher than the radar estimates. Biases for the optically thick regions ranged from +500 m to +800 m. In optically thin areas of cloud the radar height was higher than the satellite-derived heights with biases ranging from -2500 m to -2000m.

5.2. Spatial Coherence Method vs. Radar

Results and error calculations for the 2 Nov case using spatial coherence were an improvement over the black body method. Using the same radar cloud top algorithm as

in the black body comparisons, the spatial coherence method was able to detect and determine cloud top height with more accuracy even when the cloud became optically thin. The spatial coherence determined value of Lcld ranged from 54.0 to 55.5 W/m^2 sr^{-1} cm^{-1} during the course of the life cycle of the cloud. This resulted in a cloud top height of 5700 - 5400 meters. The spatial coherence mean for the cloud top in the scene never went below the radar-derived height during the life cycle of the cloud. This shows the strength of the spatial coherence method in detecting optically thin clouds. The main drawback of the spatial coherence method is its lack of cloud structure in the height retrieval. There is only one value of cloud top height for the entire cloud scene. This limits the use of spatial coherence to small horizontal scales. Biases ranged from +700 to +900 m.

During the 14 Oct case. The spatial coherence method yielded cloud tops in the range of approximately 5900 m to 6200 m during the lifecycle of the cloud with a drop in cloud top late in period (~1715Z) to about 5400m. Similar to the 2 Nov case, the spatial coherence cloud tops were usually higher than the radar estimates. Biases ranged from +250 m to +850 m. The largest errors occurred when the cloud top was not uniform. This was due to the slightly convective nature of the cloud early in the period. This can be seen in the Fig 5.1.

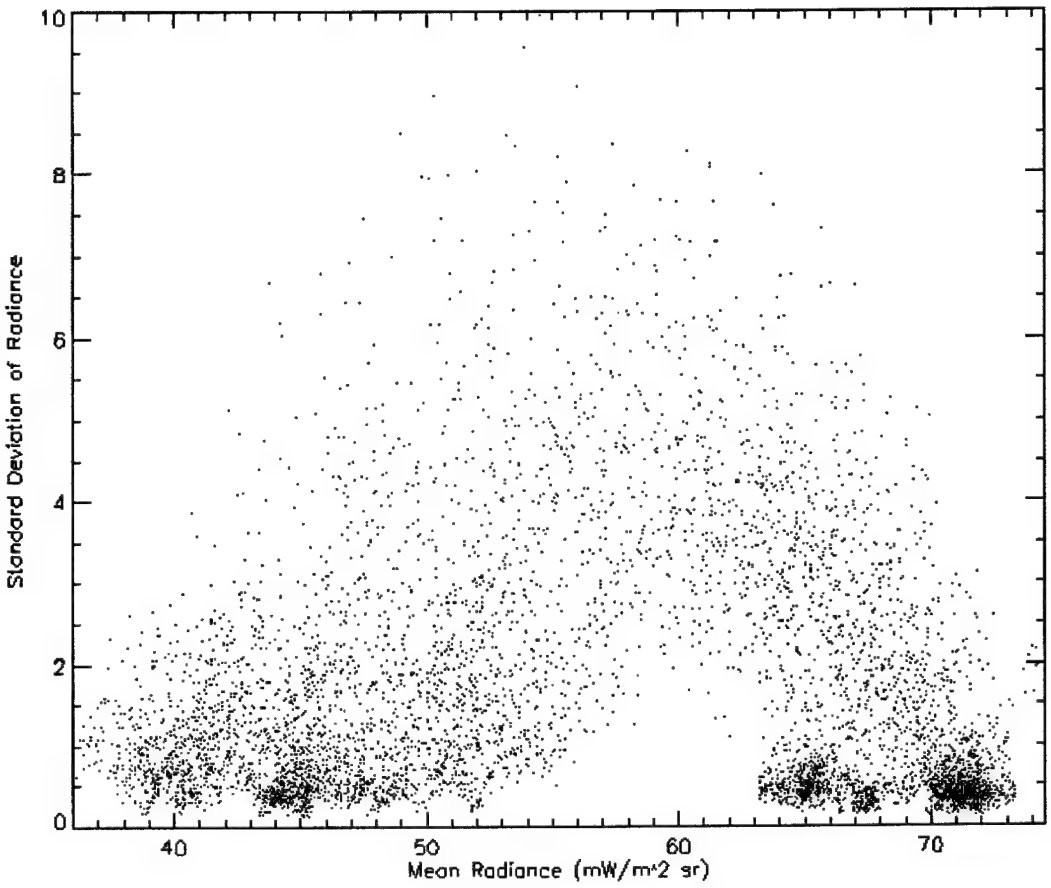

Figure 5.1. Spatial Coherence Diagram – 14 Oct 01 1245Z

This figure shows no clear determination of Lcld due to the highly variable cloud tops. Instead, several possibilities exist for the value of Lcld. This is an instance where spatial coherence fails to accurately determine the structure of the cloud. Since spatial coherence only returns one value of height for each cloud scene, large variations in vertical structure yield large errors in cloud top height. Late in the period, the cloud was more flat and the spatial coherence mean more closely resembled the cloud top height, even in areas where the cloud was not optically thick.

Biases for the spatial coherence derived cloud tops ranged from +700 m to +900 m on the 2 Nov case and +300 m to +850 m on 14 Oct. The spatial coherence method

showed only slight dependence on the opaqueness of the cloud. The reason for this is the strength of the spatial coherence method in locating radiatively significant portions of the cloud and using them to determine the height for the entire cloud field. Because these clouds are stratiform in nature only a small fraction of the FOVs need to be opaque to determine a height for the entire cloud field. This makes this an excellent method to determine cloud top height for these types of clouds. However, constraints of the method limit its use to simple cloud fields and small horizontal scales.

5.3. Optimal Estimation vs. Radar

Using optimal estimation, as described in chapter 4 and the same radar cloud top algorithm as before, significant improvement in cloud top height determination was noted. The optimal estimation algorithm used radiance values from the black body method and the values of Lcld from the spatial coherence method. Biases of each were used to determine the respective variances. The effective cloud amount threshold was .4 as determined by the histograms of N'. During the 2 Nov case, the results of the optimal estimation method yielded cloud top heights of 4500 - 5200 meters. The cloud top heights were generally higher than the radar derived cloud top until the cloud was extremely thin. This was due to the influence of the spatial coherence component in the measurement calculations and its ability to detect optically thin clouds. Biases ranged from +200 to +400 m. The A parameter, which describes the dependence of the retrieval on the 'a priori' estimate, was generally about .96 which showed a strong reliance on the measurement opposed to the a priori value of height chosen from the North Platte sounding (4.8 km). The value of the A parameter could be adjusted by forcing a smaller

variance on the a priori value (1 km was used). The value of χ^2 remained less than 1 for all the retrievals indicating a good result. The error covariance ranged from ~ 27 to 32.5 meters which is smaller than the error assumed for the satellite system.

The results of error calculations for the 14 Oct 01 case were similar. The effective cloud amount threshold used was .3 to .4 as determined by the histograms of N'. The optimal estimation method yielded cloud top heights between 4000 - 6200 meters. As in the 2 Nov case, the cloud top heights were generally higher than the radar derived cloud top until the cloud was extremely thin. Biases ranged from +200 to +700 m in FOVs where the cloud was optically thick. However, in some instances the cloud was so optically thin (N' < .3), the N' threshold prevented the algorithm from calculating a height even though hydrometeors were evident on radar. This shows the limit at which remote sensing of cloud top height by satellites is not practical.

As in the 2 Nov case, the A parameter on 14 Oct was generally about .96 which showed a strong reliance on the measurement opposed to the a priori value of height chosen from the North Platte sounding (5.5 km early then 5.0 km late). The value of χ^2 remained less than 1 for most of the retrievals indicating good results. The error covariance was ~ 40 m for good retrievals.

CHAPTER 6 – OPPORTUNITIES FOR IMPROVEMENT

Opportunities for improvement in detecting cloud top height abound. The following are some ideas of where improvements can be made.

6.1. Weighting the optimal estimation inputs by the effective cloud amount.

Instead of using N' as a threshold for the use of the optimal estimation algorithm, it can be used as a weighting factor. A study to relate the error in cloud top height to the effective cloud amount would be necessary to ensure the variances are calibrated to the value of N'. The method could possibly extend the ability to detect more optically thin ($N' < .4$) cloud layers.

6.2. Use of optimal estimation with sounder data opposed to imager data.

With the use of additive sounder channels (wavelengths), more be available to the optimal estimation algorithm. This would allow for a vector weighting function instead of the scalar form used in this study and possibly increase the vertical resolution and thereby increasing the accuracy of cloud top height determination.

6.3. Incorporation of multiple scattering into Forward Function of Optimal Estimation.

Emission and absorption are only part of all the physics involved in radiative transfer. Inclusion of scattering would result in more accurate height determinations.

REFERENCES

Baumgardner, D., 1989: Airborne Measurements for Cloud Microphysics. *NCAR Research Aviation Facility Bulletin*, **24**, 1-22.

Carey, L. D., T. H. Vonder Haar, J. A. Kankiewicz, J. M. Davis, J. M. Foresythe, D. L. Reinke, K. E. Eis, R. P. Flieishauer, and V. E. Larson, 2001: An Overview of the Next Complex Layered Cloud Experiment (CLEX-9). Proceedings CD, Battlespace Atmospheric and Cloud Impacts on Military Operations (BACIMO) 2001 Conference, July 10-12, Fort Collins, CO (ARL), 6 pp.

Chen, M., R. B. Rood, J. Joiner 1999: Assimilating TOVS Humidity into the GEOS-2 Data Assimilation System. *J. Climate*, **12**, 2983-2995.

Clothiaux, E. E., K. P. Moran, B. E. Martner, T. P. Ackerman, G. G. Mace, T. Uttal, J. H. Mather, K. B. Widener, M. A. Miller, D. J. Rodriguez, 1999: The Atmospheric Radiation Measurement Program Cloud Radars: Operational Modes. *J. Atmos. Oceanic Technol.*, **16**, 819-827.

Coakley, J. A., F. P. Bretherton, 1982: Cloud Cover From High-Resolution Scanner Data: Detecting and Allowing for Partially Filled Fields of View. *J. Geophys. Res.*, **87,** 4917-4932.

Engelen, R. J., G. L. Stephens, 1997: Infrared Radiative Transfer in the 9.6um Band: Application to TIROS Operational Vertical Sounder Ozone Retreival. *J. Geophys. Res.*, **102**, 6929-6940.

Fleishauer, R. P., 2001: Observed Microphysical Structure of Mid-Level, Mixed-Phase Clouds. PhD Dissertation, CSU, 176 pp.

Fleishauer, R. P., V. E. Larson, J. A. Kankiewicz, D. L. Reinke, T. H. Vonder Haar, 2000: Complex Layered Cloud Experiment (CLEX –5): Preliminary Phenomenology of Four Case Studies. Battlespace Atmospheric and Cloud Impacts on Military Operations (BACIMO) 2000 Conference, April 25-27, Ft Collins, CO., 12 pp.

Glahn, H. R., 1966: On the Usefullness of Satellite Infrared Measurements in the Determination of Cloud Top Heights and Areal Coverage, *J. Appl. Meteor.*, **5**, 189–197.

Joyce, R., J. Janowiak, G. Huffman, 2001: Latitudinally and Seasonally Dependent Zenith-Angle Corrections for Geostationary Satellite IR Brightness Temperatures. *J. Appl. Meteor.*, **40**, 689–703.

Larson, V. E., R. P. Flieishauer, J. A. Kankiewicz, D. L. Reinke, and T. H. Vonder Haar, 2001: The Death of an Altocumulus Cloud. *Geophys. Res. Lett.*, **28**, 2609-2612.

Larson, V. E., R. P. Fleishauer, J. A. Kankiewicz, D. L. Reinke, T. H. Vonder Haar, 2000: An Observational Study of the Microphysics of Altostratus Clouds. Battlespace Atmospheric and Cloud Impacts on Military Operations (BACIMO) 2000 Conference, 25-27 April, Ft. Collins, CO., 10 pp.

Menzel, W. P and J. W. Purdom, 1994: Introducing GOES-I: The First of a New Generation of Geostationary Operational Environmental Satellites. *Bull. Amer. Meteor. Soc.*, **75**, 17-67.

Nieman, S. J., J. Schmetz, W. P. Menzel, 1993: A Comparison of Several Techniques to Assign Heights to Cloud Tracers. *J. Appl. Meteor.*, **32**, 1559-1568.

Pazmany, A., J. Mead, R. McIntosh, 1994: 95-GHz Polarimetric Radar Measurements of Orographic Cap Clouds. *J. Atmos. Oceanic Technol.*, **11**, 140-153.

Paluch, I. R., C.A. Knight, L. J. Miller, 1996: Cloud Liquid Water and Radar Reflectivity of Nonprecipitating Cumulus Clouds. *J. Atmos. Sci.*, **53**, 1587-1603.

Rodgers, C. D., 1990: Characterization and Error Analysis of Profiles Retrieved From Remote Sounding Measurements. *J. Geophys. Res.*, **95**, 5587-5595.

Vali, G., S. Haimov, 2001: Observed Extinction by Clouds at 95 GHz. *IEEE Trans. Geoscience and Remote Sensing*, **39**, 190-193.

Vonder Haar, T. H., S. K. Cox, G. L. Stephens, J. M. Davis, T. L. Schneider, W. A. Petersen, A. C. Huffman, K. E. Eis, D. L. Reinke, and J. M. Forsythe, 1997: Overview and Objectives of the DoD Center for Geosciences Sponsored "Complex Layered Cloud Experiment" (CLEX). Proceedings, 1997 Battlespace Atmospherics Conference, 2-4 December, San Diego, CA.

Warren, S. G., C. J. Jahn, J. London, R. M. Chervin, and R. Jenne, 1988: Global Distribution of Total Cloud Cover and Cloud Type Amount Over Land. NCAR Tech. Note TN-317 STR, 212.

Weinreb, M. P., M. Jamieson, N. Fulton, Y. Chen, J. X. Johnson, J. Bremer, C. Smith, and J. Baucom, 1997: Operational Calibration of Geostationary Operational Environmental Satellite-8 and -9 Imagers and Sounders. *Appl. Optics*, **36**, 6895-6904.

Wylie, D. P., W. P. Menzel, 1989: Two Years of Cloud Cover Statistics Using VAS. *J. Climate*, **2**, 380-392.

BLANK PAGE

APPENDIX A

OPTIMAL ESTIMATION

This approach to optimal estimation is derived from the method described in Rodgers (1990) and follows closely the method explained in Engelen and Stephens(1997). It starts with a measurement, y, and a forward function, F(x), which describes some radiance value as a function of height, x, such that:

$$y = F(x) + \varepsilon$$

where ε represents the error in the measurement system. The measurement in this case is the 10.7 um radiance value (L_{ch4}). It is combined with the spatial coherence mean (L_{cld}) for cloudy FOVs in the scene. The two values were combined as independent measurements using the reciprocal of the square of the standard deviations as a weight:

$$y = \frac{L_{ch4}/\sigma_{ch4}^2 + L_{cld}/\sigma_{sc}^2}{1/\sigma_{ch4}^2 + 1/\sigma_{sc}^2}$$

The variances for each measurement were determined by the results of cloud top comparisons of the two methods to radar data. This combination of measurements was only performed in FOVs that exceeded a threshold value of N'. When a FOV contained less than 4/10 cloud coverage, i.e. N' less than .4, the routine returned a 'not retrievable' flag. In this case, the Ch 4 radiance value represents the surface radiance (or moist layers close to the surface) and no height retrieval was meaningful.

The forward function, F(x), used in this method was a two-step process consisting of a linear interpolation of height to temperature and then converting the value to a radiance with the Planck function. The conversion from height to temperature was performed using a typical mid-latitude, summer sounding (see Appendix B) that had been adjusted to match a local sounding. This typical sounding was free from inversions that can cause difficulties in proper vertical placement of clouds. After converting height to a temperature, the GVAR Planck function was used to convert the temperature to a brightness temperature and finally radiance.

An initial value of cloud top height is necessary to start the algorithm. This a priori value, x_a, was chosen from the sounding near the cloud under scrutiny. The cloud layers were chosen from the height of the temperature and dew point fields where clouds seemed apparent. The variance of this height was made sufficiently large to account for spatial and temporal variations during the day.

With all these elements in place, the algorithm was started for the cloud scene. The weighting function, which is defined as $K = \partial F / \partial x$, was calculated using a simple perturbation method:

$$K = \frac{\mathrm{F}(1.01\hat{x}) - \mathrm{F}(0.99\hat{x})}{0.02\hat{x}}$$

Then a new value of x was calculated using:

$$x^{i+1} = \frac{S_a^{-1}x_a + KS_y^{-1}(y - F(x^i) + Kx^i)}{S_a^{-1} + K^2 S_y^{-1}}$$

and the error covariance of the current value of x was found using:

$$S_x^{-1} = S_a^{-1} + K^2 S_y^{-1}$$

The algorithm repeated until a convergence criterion was met. The convergence test used was:

$$\frac{(x^{i+1} - x^i)^2}{S_x} < .01$$

Once the convergence criterion was met, the value of the height was assigned to the FOV. The A parameter and χ^2 were calculated for each FOV as well. The A parameter was calculated using:

$$A = 1 - \frac{1}{1 + K^2 \frac{S_a}{S_y}}$$

The A parameter was used to diagnose the dependence of the retrieval on the specified a priori cloud top height. The a priori estimate was given a large variance to ensure a heavy reliance on the measurement.

χ^2 was found by using:

$$\chi^2 = \frac{(y - F(x^i))^2}{S_y} + \frac{(x_a - x_i)^2}{S_a}$$

A moderately good retrieval would have $\chi^2 \sim 1$ according to Engelen and Stephens (1997).

This process was repeated for all the FOVs in the scene. The result was an array of cloud top heights. The following is the IDL code used for the optimal estimation algorithm.

```
PRO optimal_estimation_and_radar
; This program uses optimal estimation to determine the cloudtop
; using an initial cloud top height from an a priori sounding, ch4 GOES radiance
; measurement and ch4 Spatial Coherance measurement of cloudtop radiance.

;*************************************************************************
; set up video for plotting
set_plot, 'win'
device, decompose = 0
loadct,0
tvlct, 255,255,255,255
!P.background = 255
!P.color = 0

;*************************************************************************
; Read in sat data
filename=DIALOG_PICKFILE(PATH='C:\Satellite\GOES8',FILTER='2001306*.c04')
read_MCIDAS, filename,all_lat,all_lon,all_rad,all_btp
date_time_stamp = STRMID(filename,28,7)

;*************************************************************************
;Read in WCR data (netCDF format).....
filename = 'C:\jim\radar data\Wpp01-11-02-12-14-09.SPPmag.ncp'
read_radar, filename, hh_1hz, radar_range,time,glat,glon,galt,hpitch,hroll
;*************************************************************************
; Define time to consider and trim arrays
scan1 = where(time EQ 131123)
scan2 = where(time EQ 132500)

time = time(scan1:scan2)
glat = glat(scan1:scan2)
glon = glon(scan1:scan2)
alt = galt(scan1:scan2)
galt = galt(scan1:scan2)
hpitch = hpitch(scan1:scan2)
hroll = hroll(scan1:scan2)
;*************************************************************************
; Plot satellite Image and select cloud scene
window,0
X = [-.5, -.5, .5, .5, -.5]
Y = [-.5,  .5, .5, -.5, -.5]
USERSYM, X, Y,/fill

MAP_SET, 40,-100, 0, limit = [35,-110,46,-93],/mollweide,/USA,title ='CH 4 Radiance '
+ date_time_stamp + ' with Cloud Scene'
plots, all_lon, all_lat,color= 255 - bytscl(all_rad),psym=8
```

```
MAP_SET, 40,-100, 0, limit = [35,-110,46,-93],/mollweide,/USA,/noerase,/noborder,$
color = 255
oplot, glon,glat

;***********************************
; Define sector containing cloud
low_lat = 39.5
high_lat = 42.5
left_lon = -104.
right_lon = -97.

cloud_scene = where((all_lat GT low_lat AND all_lat LT high_lat) AND (all_lon GT
left_lon AND all_lon LT right_lon ))

ch4rad = all_rad(cloud_scene)
ch4lat = all_lat(cloud_scene)
ch4lon = all_lon(cloud_scene)
ch4btp = all_btp(cloud_scene)


;*************************************************************************
; Insert radiances from SC (known from previous calculations
Lcld = 47.5                    ; W/m^2 sr cm^-1
Lclr = 94.
;*************************************************************************

;calculate N' and develop histogram

N = (ch4rad - Lclr)/ (Lcld - Lclr)

hist = HISTOGRAM(N,binsize=.1,max=2.,min=-2.)
bins = FINDGEN(N_ELEMENTS(hist))/10 - 2.
PRINT, MIN(hist)
PRINT, bins

;*************************************************************************
; Plot Histogram of N'
window,1
PLOT, bins, hist, PSYM = 10,xs=1, xrange = [-.5,1.5],title = 'Histogram of Effective
Cloud Amount',$
      XTITLE = 'Bin Value', YTITLE = 'Density per Bin',subtitle = date_time_stamp
```

```
;*************************************************************************
; Combine measurements
SC_S = 1.5
rad_S = 2.
rad_S = rad_S ^2
SC_S = SC_S ^2

rad = ch4rad
sigma_rad = ch4rad

these = where(N GT .4,complement = others)

sigma_rad(these) = 1/(1/rad_S + 1/SC_S)
rad(these) = sigma_rad(these) * (ch4rad(these)/rad_S + Lcld/SC_S)

sigma_rad(others) = rad_S
rad(others) = ch4rad(others)

;*************************************************************************
; Read in Sounding Data
filename = 'C:\jim\Radiosonde\200130612z.txt'
read_NWS_radiosonde, filename, htd

htd(1,*) = htd(1,*) + 1.  ; correct sounding to match in-situ measurement

;*************************************************************************
;This reads in a midlatitude summer atmosphere profile from mls.dat
mls = fltarr(6,61)
readf,1, mls
close, 1

mls_height = reform(mls(0,*))
mls_temp = reform(mlw(2,*)) - 12.  ; correct sounding to match NWS sounding

window, 2
plot, mlw_temp,mlw_height*1000.,yrange = [0,8000],xrange = [240,300]
oplot, htd(1,*),htd(0,*)

;*************************************************************************
;This is the begining of the process to retreive the cloudtop height

Xa = 5.
Sa = (1.0)^2
Sy = sigma_rad
y = rad
retrieved_height = fltarr(N_ELEMENTS(y))
```

```
Sx_array = fltarr(N_ELEMENTS(y))
A = fltarr(N_ELEMENTS(y))
Chi_sq = fltarr(N_ELEMENTS(y))

bad_index = 0
converge = 3.
counts = 0
FOR i= 0, N_ELEMENTS(y) -1 DO BEGIN
x = Xa
IF rad(i) LT 100. THEN BEGIN
WHILE converge GT .01 DO BEGIN
K = (Forward_Model(1.01*x,mlw_height,mlw_temp) -
Forward_Model(.99*x,mlw_height,mlw_temp))/.02/x
new_x = (Xa/Sa + K/Sy(i)*(y(i) -
Forward_Model(x,mlw_height,mlw_temp)+K*x))/(1/Sa + (K^2)/Sy(i))
Sx = 1/(1/Sa + K^2/Sy(i))
converge = ((new_x - x)^2)/Sx
x = new_x
counts = counts + 1
if counts GT 5 then begin
bad_index = [bad_index,i]
converge = .001
x=0.
endif
ENDWHILE
ENDIF ELSE BEGIN ; rad
x = 0.
Sx = 0.
ENDELSE

retrieved_height(i) = x
A(i) = 1- (1/(1+(K^2)*Sa/Sy(i)))
chi_sq(i) = (y(i)- Forward_Model(x,mlw_height,mlw_temp))^2/Sy(i) + ((Xa - x)^2)/Sa
Sx_array(i) = Sx
counts = 0
converge = 3.
ENDFOR

retrieved_height = retrieved_height *1000.          ; convert from Km to meters
;*************************************************************************
; perform nearest neighbor routine to match satellite and radar data sets

x=N_ELEMENTS(time)
nn_OE_height = fltarr(x)
nn_Sx = fltarr(x)
nn_A = fltarr(x)
```

```
nn_Chi_sq = fltarr(x)
nn_sat_lat = fltarr(x)
nn_sat_lon = fltarr(x)


FOR i = 0L, x-1 DO BEGIN
lon_diff = abs(ch4lon - glon(i))
lat_diff = abs(ch4lat - glat(i))
least_square = SQRT((lon_diff)^2 + (lat_diff)^2)
point_index = where(least_square EQ min(least_square),count)      ; find shortest distance
if count EQ 1 then begin
nn_OE_height(i) = retrieved_height(point_index)
nn_sat_lat(i) = ch4lat(point_index)
nn_sat_lon(i) = ch4lon(point_index)
nn_Sx(i) = Sx_array(point_index)
nn_A(i) = A(point_index)
nn_Chi_sq(i) = Chi_sq(point_index)
endif else begin
endelse
ENDFOR

window,3
plot, glon,glat,yrange = [40,43],psym=3,xtitle = 'Longitude (degrees)',ytitle = 'Latitude
(degrees)'
oplot, nn_sat_lon,nn_sat_lat,psym = 6

;*************************************************************************
; make radar array that is corrected for a/c altitude and range gate spacing

radar_array = transpose(hh_1hz(*,scan1:scan2))
radar_heights = fltarr(N_ELEMENTS(time),N_ELEMENTS(radar_range))
FOR i = 0, N_ELEMENTS(radar_range) -1 DO BEGIN
radar_heights(*,i) = galt + radar_range(i)
ENDFOR

; this section corrects height for pitch and roll
radar_heights_pitch_roll = radar_heights
FOR i = 0,N_ELEMENTS(time)-1 DO BEGIN
FOR j = 0,N_ELEMENTS(radar_range) - 1 DO BEGIN
radar_heights_pitch_roll(i,j) = galt(i) +
radar_range(j)*SQRT((COS(hpitch(i)*!PI/180))^2 + (COS(hroll(i)*!PI/180))^2 - 1)
ENDFOR
ENDFOR
```

```
;*************************************************************************
; Determine Cloud Top Height by Radar
threshold = -20.
radar_top = fltarr(N_ELEMENTS(time))
FOR i = 0,N_ELEMENTS(time)-1 DO BEGIN
these = where(radar_array(i,*) LT threshold AND radar_heights_pitch_roll(i,*) GT
4000.)
if these(0) NE -1 then begin
radar_top(i) = radar_heights_pitch_roll(i,these(0))
endif else begin
radar_top(i) = radar_top(i-1)
endelse
ENDFOR

;*************************************************************************
; Calculate RMS error in satellite heights

RMS = SQRT(mean((nn_OE_Height - radar_top)^2))


; *******Plot satellite image with height represesenting color **********
X = [-.5, -.5, .5, .5, -.5]
Y = [-.5,  .5, .5, -.5, -.5]
USERSYM, X, Y,/fill

window,4
MAP_SET, 40,-100, 0, limit = [35,-110,46,-93],/mollweide,/USA,title ='OE Cloud
Height -' + date_time_stamp
plots, all_lon, all_lat,color= 255 - bytscl(all_rad),psym=8

;*************************************************************************

plots, ch4lon, ch4lat,color= bytscl(retrieved_height,max=8000,min=2000,top =
253)+1,psym=8
MAP_SET, 40,-100, 0, limit = [35,-110,46,-93],/mollweide,/USA,/noerase,/noborder,
color = 255
oplot, glon,glat
colorbar,position = [.1,.05,.9,.08],divisions = 8,bottom= 1,ncolors = 253,range =
[2000,8000], title='meters'

;*************************************************************************
; Create plots with radar and satellite derived heights
bottom = 2000
top = 8000
xaxis = indgen(N_ELEMENTS(time))
```

```
window, 5
plot, xaxis, galt, position = [.1,.1,.85,.9],xs=1,xr = [-10,max(xaxis)],yr =
[bottom,top],/NODATA,ytitle = 'Height(meters)',$
            xtitle = Date_Time_stamp + ' Aircraft Position Number / Seconds)'
FOR i = 0,N_ELEMENTS(galt) - 1 DO BEGIN
plots, i,radar_heights_pitch_roll(i,*), color = bytscl(radar_array(i,*), MIN=-40, MAX =
15)
ENDFOR
Colorbar, position = [.95,.1,.97,.9],/vertical,divisions = 6,bottom= 0,ncolors = 256,range
= [-40.,15.], Format = '(I3)', Title = 'Reflectivity Values in dBz!X'
oplot, nn_OE_height,color = 0
;oplot, radar_top, color =255


window,6
plot, nn_Sx*1000., xs = 1,xr = [0,max(xaxis)],title = 'Error Covariance (Sx) ' +
date_time_stamp,$
    xtitle = Date_Time_stamp + ' Aircraft Position Number / Seconds)',ytitle = 'meters'

window,7
plot, nn_A,xs = 1,xr = [0,max(xaxis)],yr = [0,1],title= 'Value of A Parameter ' +
date_time_stamp,$
      xtitle = Date_Time_stamp + ' Aircraft Position Number / Seconds)',ytitle = 'A'

window,8
plot, nn_Chi_sq,xs = 1,xr = [0,max(xaxis)], title = 'Value of Chi Squared ' +
date_time_stamp,$
 xtitle = Date_Time_stamp + ' Aircraft Position Number / Seconds)',ytitle = 'Chi Squared'

;*********************************************************************
; Plot comparison of heights with difference and RMS

subtitle = date_time_stamp + '   RMS error =' + strmid(string(RMS),5,6) + ' meters'
window,9
plot, nn_OE_Height,yrange =[-1000,8000],title = 'Radar vs Optimal Estimation Derived
Heights',subtitle =subtitle,$
           xtitle = 'Aircraft Position Number / Seconds',ytitle = 'Height (meters)'
oplot,radar_top,color= 200
oplot, nn_OE_Height - radar_top,color = 75

END

;*********************************************************************
```

```
;*********************************************************************
function Forward_Model,ct_height,mlw_height,mlw_temp
; This function uses a cloudtop height to calculate a GOES-8 Ch4 radiance value.
;  It uses a Midlatitude Summer Atmosphere to convert cloudtop height(m) to
;  temperature (K)
;  Then uses NOAA's GCAL method to convert temperature to Tb(K) and then to
;  Radiance (mW/m^2 sr (cm^-1))

;Define constants
FK1 = 9737.93
FK2 = 1345.37
TC1 = .3735
TC2 = .9987
;*************************************************************
ct_temp = INTERPOL(mlw_temp,mlw_height,ct_height)

Tb = TC2*ct_temp + TC1

;McIDAS Planck function
rad = FK1/(exp(FK2/Tb) - 1.)

return, rad
END ; Forward Model
```

APPENDIX B

METEOROLOGICAL SOUNDINGS

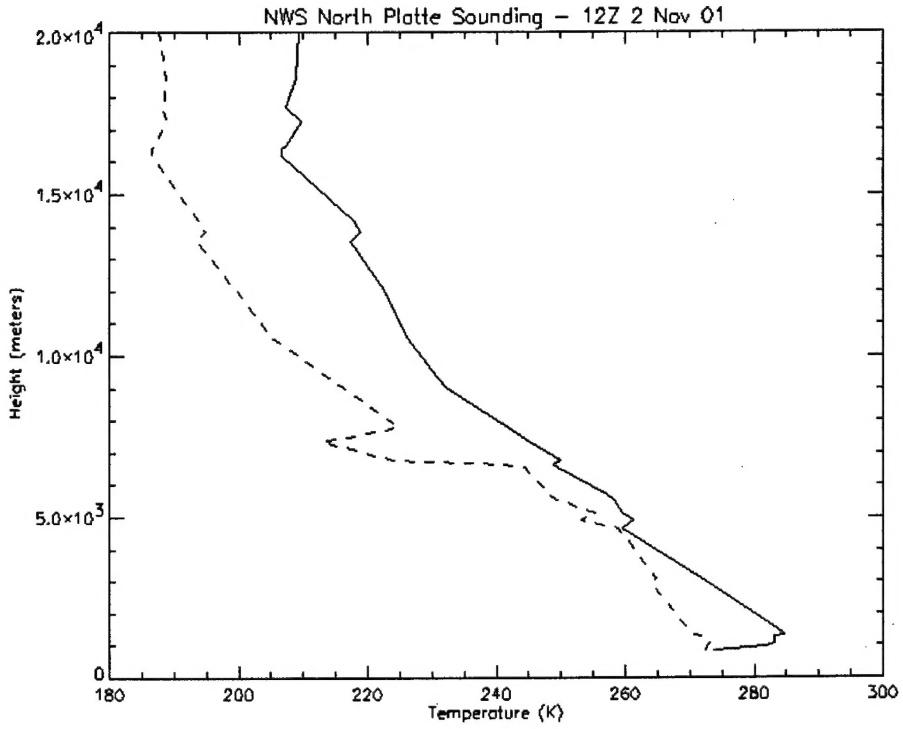

Figure B.1. North Platte Sounding - 12Z 2 Nov 01

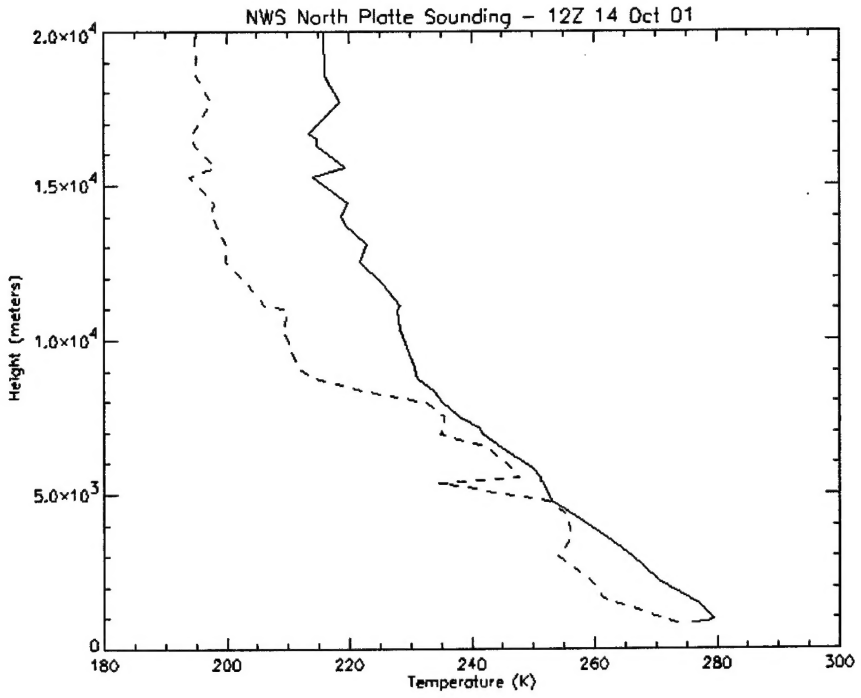

Figure B.2. North Platte Sounding - 12Z 14 Oct 01

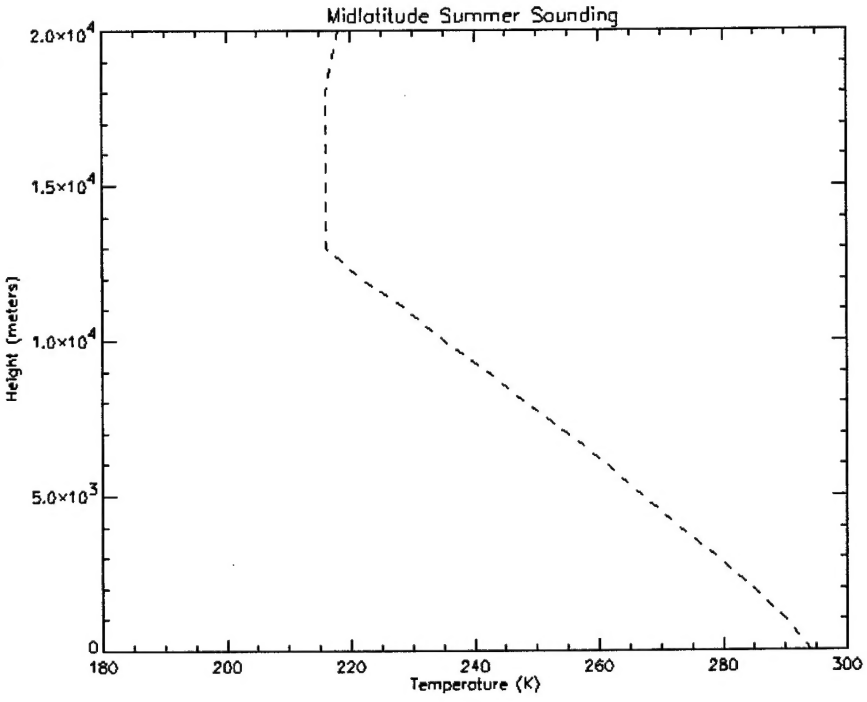

Figure B.3. Midlatitude Summer Sounding